Dynamic Demulsification Mechanism of Asphaltene-Stabilized Water-in-Oil Emulsions by Ethylcellulose

by

Yin Liang

A thesis submitted in partial fulfillment of the requirements for the degree of

Master of Science

in

Chemical Engineering

Department of Chemical and Materials Engineering

University of Alberta

© Yin Liang, 2015

Abstract

In previous studies, nontoxic and biodegradable ethylcellulose (EC) was shown to be capable of breaking water-in-diluted bitumen emulsions. Nevertheless, the demulsification mechanism of EC has not been correlated to its effect on the physical properties of stabilizing interfacial asphaltene films. In this study, the effect of EC addition on rheological properties and morphology of heptol diluted asphaltene-water interfacial films was investigated. The adsorption kinetics of asphaltenes and EC at oil-water interface showed that EC was able to compete with the asphaltenes at the interface and fracture the interfacial asphaltene films. The fracture of asphaltene films enhanced coalescence and dewatering, as confirmed in demulsification bottle test and droplet-droplet coalescence time experiment. The shear and compressional rheology measurements revealed that EC could significantly soften asphaltene films formed at oil-water interface, most likely as a result of disruption of the asphaltene films network as observed with Brewster angle microscopy. In conclusion, EC was proven to soften and break the asphaltene films at the oil-water interface, promoting the coalescence of water droplets and emulsion dewatering.

Preface

Some of the research conducted for this thesis forms part of a paper to be published, including chapters 3 and 4. Other chapters are based on my original work. These two chapters are co-authored and the following list indicates the contributions for each chapter.

- Chapter 1: Introduction: Original work by Yin Liang.
- Chapter 2: Literature Review: Original work by Yin Liang.
- Chapter 3 and Chapter 4: These chapters are to be submitted as a paper entitled “Dynamic Demulsification Mechanism of Asphaltene-Stabilized Water-in-Oil Emulsions by Ethylcellulose.” co-authored by Yin Liang, Erica Pensini, David Harbottle and Zhenghe Xu. Yin Liang is responsible for experimental design, data collection and interpretation as well as manuscript preparation. Erica Pensini, David Hartbottle and Zhenghe Xu supervise the work and make suggestions to the manuscript.
- Chapter 5: Conclusion and Future Work: Original work by Yin Liang.

Acknowledgements

I would like to express my deep appreciation to my supervisor Dr. Zhenghe Xu for his excellent guidance and support of the project. I would also like to thank Dr. David Harbottle for his huge help and comments on this project. I am also thankful to Dr. Erica Pensini and Dr. Zifu Li for their technical support and advice on this work.

I would like to thank Mr. James Skwarok, Ms. Lisa Carreiro and Ms. Jie Ru for their assistance with my project. I would also like to thank all members in the Oil Sands Research Group for their great help and suggestions on my work. I also want to dedicate this thesis to my parents and all my friends.

Finally I would like to thank the Natural Sciences and Engineering Research Council of Canada (NSERC) Industry Research Chair program in Oil Sands Engineering for their financial support of my research.

Table of Contents

List of Figures

Chapter 1 Introduction

1.1 Oil Sands Overview

The production of conventional and unconventional oil now needs to follow increasing demand for energy with population growth. Canada has one of the world's largest unconventional oil reserves-oil sands. The current oil sands reserves of about 167.9 billion barrels, the third largest proven crude oil reserve, underlie 140,200 km^2 in northern Alberta, Canada.[1] The first commercial operation of Great Canadian Oil Sands mine started in 1967 by Suncor Energy followed by Syncrude in 1978. Syncrude now has become the largest oil sands operator. From 21st century, more companies such as CNRL, Nexen and Shell AOSP began their oil sands operations. In 1967, only 30,000 barrels of crude oil could be produced per day and in 2012 the number of oil production from oil sands increased to 1.8 million barrels per day.[2-3] By 2022 the overall raw crude oil production is projected to be 3.8 million barrels per day.[4]

Oil sands ores have approximately 85 wt. % solids and 8-14 wt. % bitumen with small amount of water. As unconventional oil, bitumen has high viscosity and cannot be extracted by conventional methods. According to the depth of deposits, two main methods are used to recover bitumen. Crude bitumen near the surface (within 75 m) can be recovered by open-pit mining extraction method. After the overburden is removed, bitumen is extracted from the minded oil sands ore using hot water as processing medium. For the materials at over 75 m depth, in-situ methods are employed since surface mining is no longer economical. In order to reduce the bitumen viscosity and to allow it to flow to a vertical or horizontal wellbore, Cyclic Steam Stimulation (CSS) and Steam Assisted Gravity Drainage (SAGD) are used as major methods. [4]

1.1.1 Surface Mining

Surface mining bitumen extraction process is shown in Figure 1-1. Oil sands ores are mined and crushed, followed by their mixing with hot water and chemical additives to liberate bitumen from sand grains. The slurry is diluted with water and fed into the gravity separation vessels and further to flotation cells to recover bitumen. The aerated bitumen separated from water and solids in the vessel will form bitumen froths, which contain 60 wt. % bitumen, 30 wt. % water and 10 wt. % solids. The bitumen froth is then fed to froth treatment plant after de-aeration to remove solids and water. In the froth treatment, solvents are used to reduce the bitumen viscosity and density so as to remove solids and water by gravity method before upgrading.

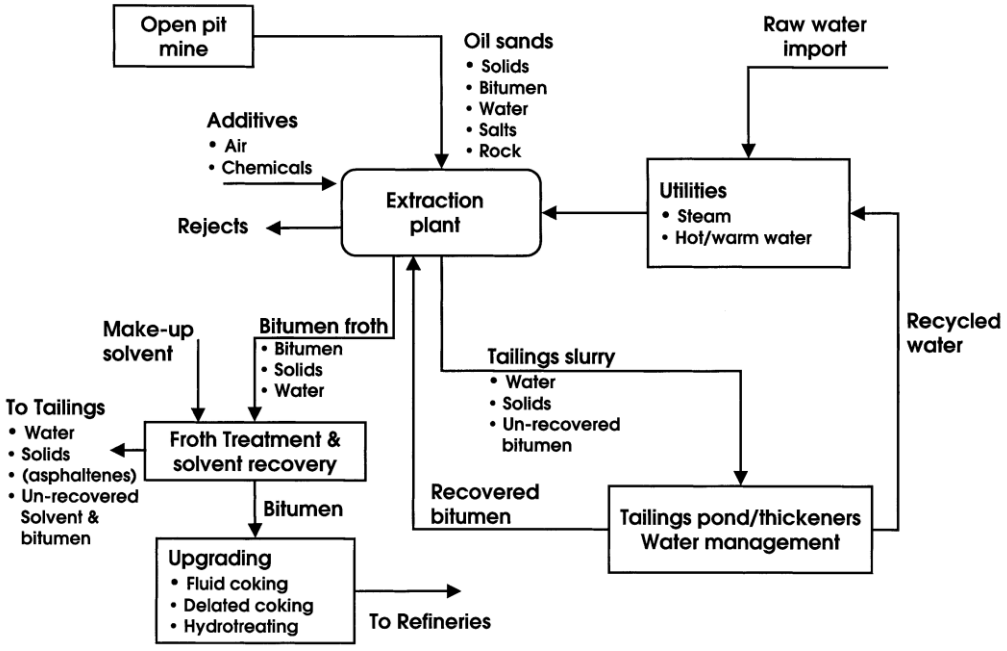

Figure 1-1 Generalized scheme for oil sands processing using surface mining.[5]

1.1.2 Steam Assisted Gravity Drainage Process (SAGD)

Whilst the potentially recoverable oil in oil sands is 315 billion barrels, only 3% of the oil sands area is mineable and the others are too deep to be mined.[6] Since 80

percent (135 billion barrels) of the oil sands are too deep for open pit surface mining, more effective underground mining techniques were being developed, while the in-situ method such as Steam Assisted Gravity Drainage (SAGD) technique was extensively used. In this technique, two horizontal wells are drilled from a central well pad and one located 4 to 6 metres above the other, as shown in Figure 1-2. Steam generated from water goes through the pipelines above ground to the underground and enters the top horizontal well. Then heavy oil is heated by the steam to a certain temperature that they can flow into the bottom well by gravity. The heavy oil is finally transported to the ground for further processing. Water is separated and treated from the emulsions and recycled for generating the new steam. The whole process is operated continuously and simultaneously.[7]

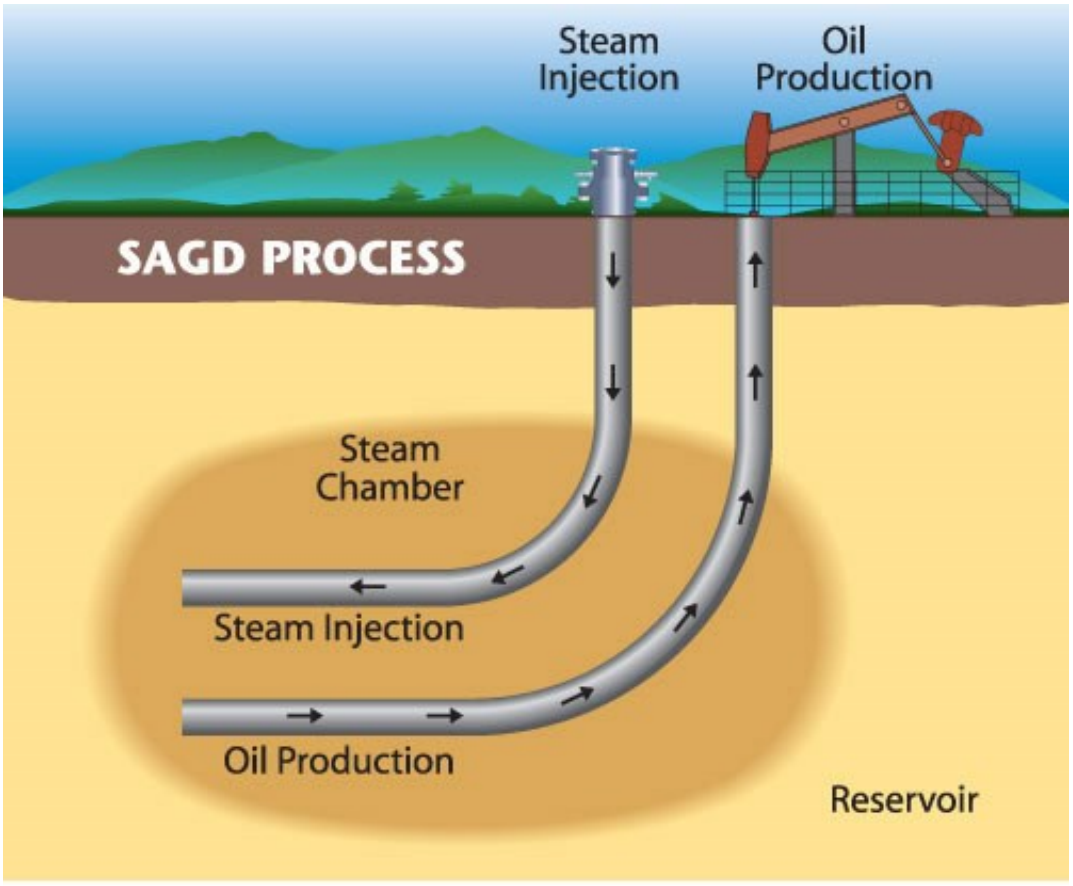

Figure 1-2 Generalized scheme for Steam Assisted Gravity Drainage Process (SAGD).[7]

1.2 Froth Treatment

In both surface mining and steam assisted gravity drainage processes, bitumen-water emulsions are obtained and call for further treatment. In the bitumen froth treatment operations, 30 wt.% aqueous and 10 wt.% solids contaminants in the bitumen froth are removed to produce a clean bitumen product (diluted bitumen). Solvents are added to separate water and solids from bitumen. In oil sands industry, there are two main methods used in froth treatments, naphthenic froth treatment and paraffinic froth treatment.

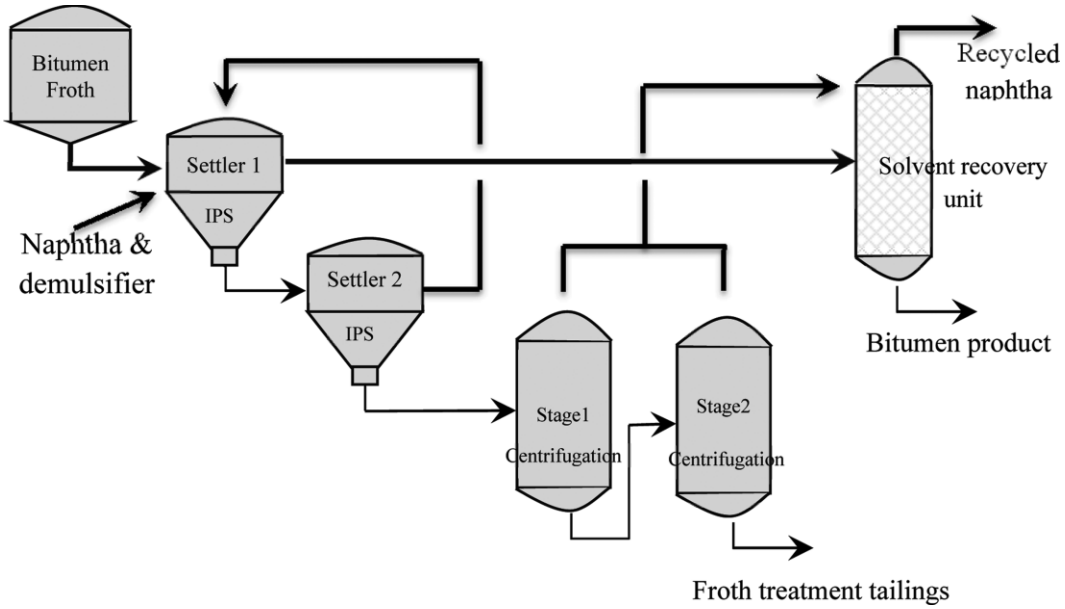

Figure 1-3 Schematics of a typical for two-stage naphthenic bitumen froth treatment process.[8]

In naphthenic froth treatment process, naphtha is chosen as the diluent (solvent), which is able to decrease the density and viscosity of diluted bitumen, to remove solids and emulsified water from bitumen froth. The diluent to bitumen mass ratio is typically around 0.7. Two stages of naphthenic froth treatment process are shown schematically in Figure 1-3. Multistage centrifugation, inclined plates settlers and hydrocyclones are applied to separating solids and water from the diluted bitumen emulsions. The whole process is performed at 80℃. However, the diluted bitumen product from naphthenic froth treatment process still contains around 2-5 wt. % water and 0.5-1 wt. % solids.[9] The chloride ions contained in residual water and the fine solids in the product may cause serious operational problems, such as corrosion of downstream process equipment, scaling and catalyst poisoning.[10-12] For these reasons, the diluted bitumen product still needs further treatment.

In paraffinic froth treatment, paraffinic diluent is added as a mass ratio of 2:1 to bitumen for viscosity and density reduction. In this process, approximately 1/3 or 1/2 of the asphaltenes is precipitated and the precipitated asphaltenes form

large aggregates with fine solids and emulsified water in the diluted bitumen. As a result, the diluted bitumen product through paraffinic froth treatment only contains ~550 ppmw (parts per million weight) to 800 ppmw solids and ~100 ppmw to 300 ppmw water. There are some challenges for paraffinic froth treatment. For instance, the asphaltene aggregates can reduce the fluidity of the underflow generated from froth treatment, which may cause pumping problems. The high solvent loss to tailings is also proven to be correlated to this type of froth treatment.[13]

In froth treatment, the residual water and solids in the diluted bitumen products are typically presented as water-in-oil emulsions. Emulsions are very common in petroleum industry, which are unavoidable and undesirable. An emulsion is a dispersed system containing two immiscible or partially immiscible liquids. Usually, one is water and the other is oil. One of these liquids presents as a continuous phase, whilst the other is dispersed into small droplets. When oil is dispersed as small droplets in continuous water phase, it will form an oil-in-water (O/W) emulsion. On the contrary, if water is dispersed in continuous oil phase, it is called water-in-oil (W/O) emulsion. The emulsion stability is caused by a thin liquid film of the continuous phase that prevents dispersed droplets from intimate contact. How to prevent the formation of water-in-oil emulsions or breaking these emulsions becomes a crucial challenge in the oil sands industry. These are three modes of destabilizing the water-in-oil emulsions: flocculation, sedimentation and coalescence.[12] Water droplets first aggregate to large aggregates/flocs (aggregation, agglomeration and flocculation), settle to the bottom of the container due to higher gravity (sedimentation) and form larger droplets until water and oil separate into two different layers (coalescence).[14] Finally, after water, solids and diluent are removed, the bitumen products are ready for the upgrading process.

1.3 Objectives and Organization of this Thesis

In previous studies, nontoxic and biodegradable ethylcellulose (EC) was shown to be an effective demulsifier capable of breaking water-in-diluted bitumen emulsions. However, the dynamic demulsification mechanism remains poorly understood. This thesis aims at understanding EC dynamic demulsification mechanism. To remove the effects of maltenes, naphthenic acids and solids, this study will focus on emulsions stabilized by asphaltenes which have been thought as the key component for stabilizing emulsions in oil industry. The effect of EC addition on rheological properties, dynamic interfacial tension, contraction behavior and morphology of heptol diluted asphaltene-water interfacial films are the main interfacial properties investigated.

In Chapter 2, a literature review of stabilization of water-in oil emulsions, the role of asphaltenes in crude oil emulsion stabilization, demulsification methods and mechanisms will be provided. In Chapter 3, the materials and experimental methods used in this thesis will be presented. Chapter 4 represents the results of the demulsification by EC on asphaltene-stabilized emulsions studied using bottle tests and drop-drop coalescence time measurement. The effect of EC on interfacial rheological properties, interfacial asphaltene film morphology, dynamic interfacial tension, interfacial pressure-area isotherms and contraction behaviour is determined and discussed. Interfacial dilatational and shear rheology of asphaltene films is compared. The effect of EC addition on dilatational rheology of the asphaltene interfacial film at oil-water interface is compared with the results of shear rheology. The conclusion and future work of this project are given in Chapter 5.

Chapter 2 Literature Review

2.1 Stabilization of Water-in-Oil Emulsions

There are four main mechanisms for emulsion stabilization: 1) the electrical double layer repulsion, 2) the steric repulsion, 3) the Gibbs-Marangoni effect and 4) the formation of rigid and cross-linked network at oil-water interface.[15] The last mechanism was the most acceptable.[16] In crude oil and bitumen processing, both O/W and W/O are undesirable and needed to be resolved because they may cause severe damages to the processing facilities or difficulties in oil/water separation.[17] Water droplets in oil can be stabilized by a variety of surface-active materials in oil. Among those components, it is clear from previous research that asphaltenes are a major component in stabilizing W/O emulsions,[11-12, 14, 16] which can be explained by the main stabilizing mechanism for W/O emulsions. The presence of the asphaltene films, as shown in Figure 2-1, and its relationship with emulsion stabilization have been extensively studied.[18] Bulk asphaltene molecules can first form aggregates with different sizes and adsorb to the interface. Then the adsorbed asphaltene aggregates can go through densification and rearrangement due to intermolecular interactions such as π orbital overlapping of aromatic rings, hydrogen bonding, charge-transfer interactions, multipolar forces and van der Waals interactions.[19] Some functional groups in asphaltene molecules can also self-aassociate to form aggregates, further promoting the formation of asphaltene films at the oil-water interface.

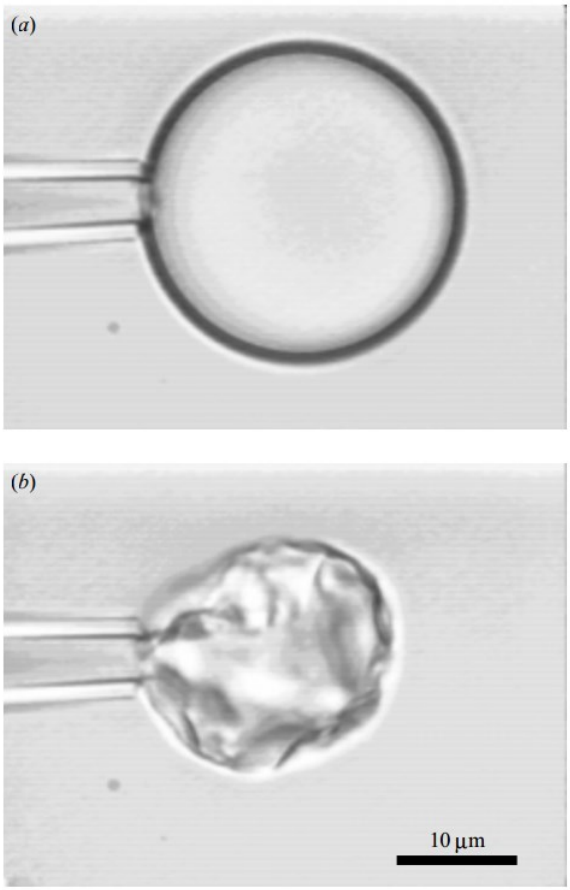

Figure 2-1 Protective asphaltene films of deflating an water emulsion drop in diluted bitumen using micropipette.[18]

In addition asphaltenes, acidic molecules such as alkyl carboxylic acids, alkylbenzene carboxylic acids, naphthenic acids and some aromatic ring acids are the other components in crude oil that are proven to be capable of stabilizing W/O emulsions. Also, some high-molecular-weight acidic species from calcium soaps are responsible for the emulsion stabilization rather than asphaltene stabilizing mechanism. These molecules can be ionized and adsorb at the oil-water interface, thus promoting the stabilization of oil-water emulsions.[15]

The fine solids and other inorganic solid particles can further enhance the stability of emulsions. The polar species in crude oil such as resins or asphaltenes adsorb on the solids and therefore modify the wettability of these solids. The

surface modified solids tend to adsorb at the oil-water interface, leading to enhanced emulsion stability. The smaller the solids, the more stable the emulsions are. The water pH and ions contained in water may also have impact on the emulsion stability.[11] Also, the formation of lamellar liquid crystalline films and smectic liquid crystalline phases are found to exit at the oil-water interface, thus the acids and their soaps are also proven to have a great impact on emulsion stability.[15]

2.2 Role of Asphaltenes in Crude Oil Emulsion Stabilization

2.2.1 Characterization of Asphaltenes

After froth treatment, bitumen products can be fractionated to saturates, aromatics, resins and asphaltenes due to different polarity and solubility, defined as SARA analysis, as shown in Figure 2-2.

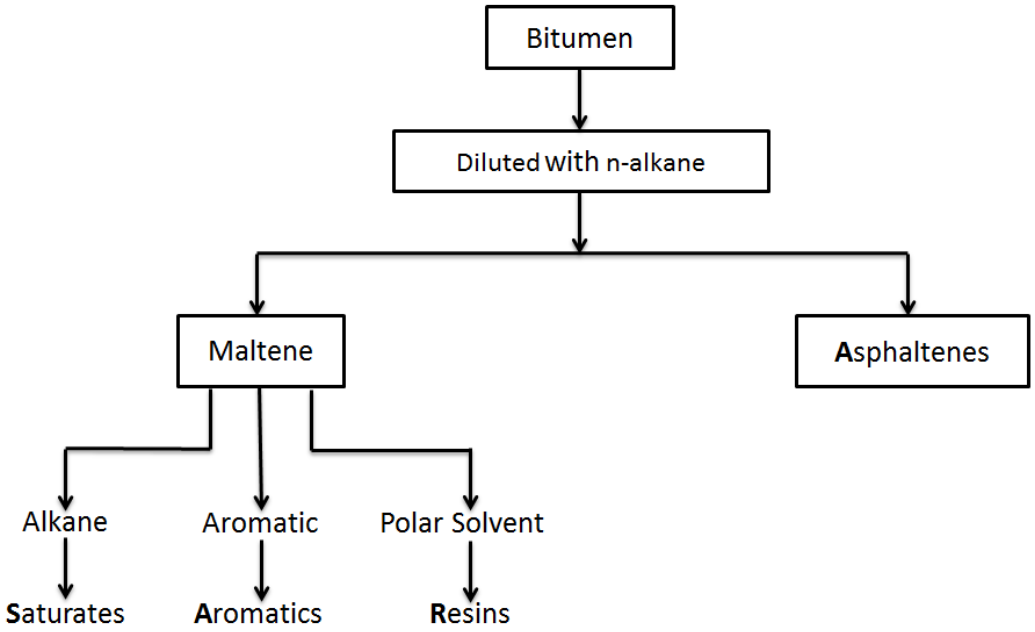

Figure 2-2 Schematic illustration of SARA analysis.

In SARA analysis, saturates, aromatics and resins are soluble in n-alkane solvents such as heptane or pentane. These mixtures are also known as maltenes. Asphaltenes are insoluble in these solvents and can precipitate and separate

from maltenes. Different methods are applied to SARA separation by different solvents and adsorbents. The amount and composition of the asphaltene precipitates depend strongly on the solvents type, the oil sample and the protocols of asphaltenes extraction.[20]

Though asphaltenes are insoluble in light alkanes, they are soluble in aromatic solvents such as toluene. Although many researchers have conducted the complex structures, chemical and physical characterisation of asphaltenes, there are still some debates on the precise structure and molecular weight of asphaltene molecules. In general, asphaltene molecular weight ranges from a few hundreds to more than a few thousands Daltons.[21-22] Most previous studies agree the range of 500-1000 Da with a mean value peaking at 750 Da.[23] Based on Nuclear Magnetic Resonance (NMR) and Infrared (IR) measurements, asphaltenes are proven to have aromatic rings with hydrogen/carbon atomic ratios of 1.0-1.2 and heteroatoms (N, S, and O) in amount from 2 to 10% (w/w). The aromatic rings in asphaltenes are also functionalized with aliphatic groups and substituted with heteroatom S-containing groups such as pyrrole, pyridine, carboxylic, quinone, thiophene, sulfhydryl, sulfonyl etc, which are capable of hydrogen bonding.[24] There are also traces (ppm) of vanadium, nickel and iron, indicating the existence of porphyrin and porphyrin-like functional groups, alkyl bridges and pendent groups.[25] According to different solvent conditions and concentrations, asphaltene molecules can form aggregates with different sizes from small oligomers to large microparticulates. The nanoscale aggregates have the size of 3-10 nm in core-shell oblate cylindrical model, as revealed by small angle X-ray scattering (SAXS) and small-angle neutron scattering (SANS).[24, 26-29] In W/O emulsions, the size of asphaltene aggregates ranges from 7-20 nm. Previous studies also show that adding n-alkane can lower the asphaltene solubility. When nanoscale aggregates are still soluble but close to precipitation under specific solvent condition, they may have the highest surface activity.[30-32] Thus in this

study, 1:1 Heptol with 50% n-heptane/ 50% toluene (v/v) is used as the solvent for asphaltenes.

2.2.2 Interfacial Properties of Asphaltenes

Based on studies using dynamic IFT, interfacial rheology, interfacial dilatational rheology, SANS, SAXS and many other techniques, P.K. Kilpatrick[15] summarized four main interfacial properties of asphaltene films at the oil-water interface 1) by molecular and intermolecular interaction, asphaltenes can rearrange their orientation with time at the interface; 2) the elasticity of the interface increases because of adequate adsorbed asphaltene molecules; 3) the dilatational elasticity correlates with the emulsion stability; and 4) the thickness of the asphaltene emulsion films ranges from 8-20 nm, whose composition has higher density than the corresponding nanoscale aggregates that comprising the film.

The stability of W/O emulsions and coalescence of water droplets in emulsions are proven to correlate with the compressibility of asphaltene interfacial films.[33-34] Interfacial shear rheology of asphaltene interfacial films appears to be viscoelastic and has yield stresses.[35] Combination of interfacial shear and dilatational rheology shows that the rearrangement and consolidation of adsorbed asphaltenes can form a "gel-like" film that dominates the stabilizing mechanism for the emulsions.[36] Other techniques such as micropipette,[37] Langmuir trough,[21, 38-39] and atomic force microscope (AFM)[40-41] also proved the presence of asphaltene films at the oil-water interface.

2.3 Demulsification Methods and Mechanisms

2.3.1 Demulsifiers

Many methods are used to break the emulsions.[38, 42] Heating (thermal methods) can reduce the viscosity of oil products and increase the rate of water settling and destabilized the rigid films due to lowered interfacial viscosity.[42] The possibility of coalescence is found to be higher at high temperature. But the

disadvantages of thermal methods are costly and may change the quality of oil products. Mechanical facilities such as free-water knockout drums, three-phase separator and de-salters are applied as mechanical methods.[43] Electrical field is also used to demulsify the W/O emulsions encountered in oil industry. When the electrical field is applied, water droplets in the emulsion will move more rapidly and be able to collide with each other and coalesce. The electric field can also weaken the interfacial film and finally facilitate droplets coalescence.[17] Compared to all the methods mentioned above, the most common method of demulsification is adding demulsifiers, which are mostly surface-active compounds. Demulsifiers are able to migrate to the oil-water interface and weaken/rupture the protective film, promoting the drop-drop coalescence. These chemical methods are the most economical and least energy consuming.[38, 44-45]

Demulsifiers can cause the drop to flocculate, disrupt the stabilized layer at the oil-water interface and further promote the drop coalescence in an emulsion. Commercially, demulsifier products usually contain several chemicals. At early time, inorganic chemicals are used, which can react with water droplets and cause them to flocculate in the emulsions.[46] Then surfactant-like polymers are introduced as dimulsifers. Nowadays a mixture of polymers and surface-active chemicals are widely used in the industry. These demulsifiers are amphiphilic compounds and are able to destabilize emulsions and change the properties of the interfacial films. The flocculent-type polymeric chemicals normally have high molecular weight and are capable of flocculating the water droplets in the emulsions. The coalescing-type demulsifiers, as interface controllers, have high interfacial activity to adsorb irreversibly at the interface, break the film and promote the coalescence of small-emulsified droplets.[47-48]

Two main factors may control the demulsification of a demulsifier: one is its amphiphilicity and the other one is the ability to break the interfacial film.[49] Wu

et al.[50] studied the effect of molecular weight of the demulsifiers on water removal from emulsions. The low molecular weight polymers such as sorbitan esters, polyoxyethylene sorbitan esters, polyoxyethylene fatty alcohol ethers and polyoxyethylene alkylphenol ethers were found to remove 20% of water at optimal dosage. However high molecular weight demulsifiers such as polymerized polyols, ethylene oxide-propylene oxide (EO/PO) copolymers and alkylphenol formaldehyde resins modified EO/PO could resolve about 90% water in the emulsions. But the most effective demulsifiers were those with intermediate molecular weight from 7500 to 15,000 Da. Zhang et al.[21] also reported that the EO/PO copolymer can weaken the asphaltene films at the oil-water interface and make the asphaltene aggregates less packed. Demulsifers with high branched structure are found to be more effective on oil-water emulsion destabilization than linear chain structure polymers.[51] Daniel-David et al. reported a triblock copolymer with branched structure-poly(alkyleneoxide)/poly(dimethysiloxane)/poly(alkylene oxide) that can break the asphatene film and promote the emulsions breakup.[52]

Among all chemical demulsifiers, EO/PO based polymers are most widely used and investigated. For EO/PO and modified EO/PO demulsifiers, the PO structure represents the hydrophobic part of the demulsifier while the EO branch contributes to the hydrophilic part. At the oil-water interface, EO chains will stay in the water droplets and PO structure will remain in the oil phase. Thus the EO/PO demulsifier is interfacially active and is able to soften and break the interfacial films in the emulsions, which are stabilized by asphaltenes and resins, etc. Many studies have correlated EO/PO demulsifier performance with the hydrophile-lipophile balance (HLB) number, relative solubility number (RSN) and their EO and PO composition.[77-79] The HLB value of EO/PO copolymer is defined as:

$$\mathrm{HLB} = \frac{\%ethoxylation}{5} \qquad (2\text{-}1)$$

The standard RSN value is calculated as the volume of water needed to be titrated with the solution of one gram of demulsifier dissolved in 30 mL of RSN solvent (benzene-dioxane solvent mixture). RSN values are proven to have linear relationship with EO numbers in the polymer. In general, the higher the RSN value, the greater hydrophilicity the polymer has.[53-54] Also, it is found that EO/PO polymers with higher branching, and higher molecular weight typically have higher demulsification efficiency.

The EO/PO demulsification mechanism of asphaltene-stabilized water-in-oil emulsions was studied by Pensini et al.[55] The interfacial tension is lowered after the addition of EO/PO demulsifiers, indicating more interfacially active nature of EO/PO demulsifers than asphaltenes. Demulsifiers are able to compete with the asphaltenes at the toluene-water interface, beneficial for breaking the interfacial film. When EO/PO demulsifier is applied, the O/C atomic ratio of the Langmuir Trough interfacial film transferred from the oil-water interface becomes higher, as determined by the X-ray Photoelectron Spectroscopy. However the value of this O/C atomic ratio is still lower than that of pure EO/PO demulsifier, showing that asphaltene molecules are only partially displaced by the EO/PO demulsifer. Since the interfacial rheological properties are correlated with the stability of the emulsions, the viscoelastic characteristics are determined as a function of aging time. Addition of demulsfier is shown to soften the asphaltene films (i.e., reduce the viscoelastic moduli of asphaltene films) under both shear and compressional interfacial deformations. Demulsifier penetration in the changes of asphaltene films the asphaltene interfacial mobility and morphology, as probed with Brewster angle microscopy (BAM) and AFM. In summary, The EO/PO demulsifiers are more interfacially active than asphaltenes at the interface and are able to partially displace the aspahltene molecules at the interface.

2.3.2 Demulsification of W/O Emulsions by Ethylcellulose

Recently, a natural polymer ethylcellulose (EC) was found effective to break the water-in-diluted bitumen emulsions.[41, 56-58] This nontoxic, biodegradable and environmentally friendly demulsifier is a commercial product and is cheap. Through bottle test, almost 90% of the water in bitumen emulsions can be resolved by EC addition. Micrographic images further reveal that EC is able to break the water-in-diluted bitumen emulsions by flocculation and coalescence.[58] In the study of demulsification mechanism of EC in diluted bitumen emulsions, micropipette technique provides the direct evidence on both flocculation and coalescence of water droplets in diluted bitumen by EC. At the molecular level, AFM images also reveal the disruption of the continuous interfacial films formed from surface-active components of bitumen by EC.[41] The addition of EC is found to decrease the naphtha-diluted bitumen/water interfacial tension significantly and disrupt the original protective interfacial films formed from the surface-active components of bitumen. Based on previous research by Hou et al., EC molecules could irreversibly adsorb at the oil-water interface, diffuse through the oil phase and form a highly compressible interfacial film.[57]

Asphaltenes have been proven to be interfacial active ingredients, which can form a rigid layer at the oil-water interface and hinder drop-drop coalescence in water-in-oil emulsions. But the dynamics of how EC affects the asphaltene stiff skin at the interface has not been fully understood. When droplets collide in an emulsion, shear and deformational modes exist, and high shear or compressional elasticity contribute to emulsion stability.[59] The relationship between the demulsifier performance and the rheology of interfacial films has been reported.[60-62] However, the rheology studies have solely been conducted to assess the effect of a non-ionic surfactant on asphaltene films, whereas the impact of EC on the shear rigidity of stabilized films is seldom reported. Although the emulsions stability by bottle tests and interfacial rheological response are

well compared, the differences between these two approaches on surface area and aging mechanisms have not been investigated.[63]

Chapter 3 Materials and Experimental Methods

3.1 Materials

3.1.1 Demulsifiers

Ethylcellulose (EC) sample with 48% ethoxyl (EC4 and EC300) was purchased from Sigma-Aldrich and used as received. The viscosity of 5 wt% EC solution in 80:20 toluene/ethanol at 25℃ is 4 mPa·s. and 300 mPa·s, respectively. The detailed structure and information of EC are shown in Figure 3-1a and Figure 3-1b. HPLC-grade n-heptane and toluene were obtained from Fishier Scientific. In this work, EC sample was dissolved in HPLC-grade toluene at the concentration of 1 mg/ml as a stock solution for 24 h prior to its use.

a)

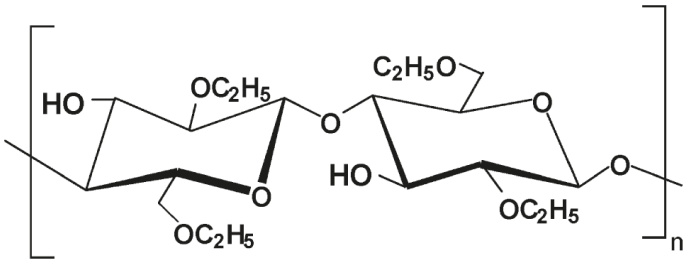

b)

Demulsifier	Ethoxyl	Molecular Weight	HLB
EC4	48%	46 kDa	7.9
EC300	48%	182 kDa	7.9

Figure 3-1 Structure of EC with a two-degree substitution (a); and detailed characteristics of Ethylcellulose (b).

3.1.2 Preparation of Asphaltene Solution

Vacuum distillation feed bitumen was provided by Syncrude Canada Ltd. The standard protocol reported in previous publications was followed.[35, 64] Vacuum distillation feed bitumen was dispersed in n-heptane at the volume ratio of 1:40. The dissolved bitumen was shaken on a shaker for 2h and equilibrated overnight

for asphaltene precipitation. The supernatant was removed and the precipitated asphaltenes were washed with fresh n-heptane at the same volume ratio for 15 times, until the supernatant became colorless. The precipitated asphaltenes were collected and dissolved in HPLC-grade toluene at the volume ratio of 20:1. Solids were then removed by centrifugation at 20,000 RCF for 30 min. The solvents in toluene-diluted asphaltenes were then removed by evaporation and the resulting asphaltenes were stored in a desiccator. The mass of the dried asphaltenes was 6.87% of the original bitumen, and the entire time of the asphaltene extraction was about 1 month. Asphaltenes extracted from bitumen were then dissolved in premixed 1:1 Heptol (volume ratio of heptane and toluene is 1:1) with 5 min sonication and the concentration of this diluted asphaltenes is 0.1 g/L. This solution (0.1 g/L asphaltenes in 1:1 Heptol) and Milli-Q® water were prepared freshly and used in all the experiments reported here.

3.2 Demulsification Performance by Bottle Test

The demulsification test was conducted to assess the potential of EC to destabilize asphaltene stabilized water-in-oil emulsions. The water-in-oil emulsions were prepared with 60 vol.% 0.1g/L asphaltenes in heptol solution (0.1g/L asphaltenes in 1:1 Heptol) and 40 vol.% water, homogenized by a PowerGen 100 homogenizer operating at 30,000 rpm for 5 min. After emulsification, 20 mL of prepared emulsions (13 cm depth in total) were transferred to a graduated cylindrical tube with a radius of 0.5 cm, where the free water volume as a function of time could be monitored. EC was added drop-wise to the emulsions at the concentration between 0.1 and 1 ppm (based on the mass of the heptol phase), and the mixture was hand-shaken for 1 min. The cylindrical tubes were then positioned vertically and the height of continuous water layer was recorded periodically to measure EC4 dewatering efficiency of the asphaltenes emulsions. Micrographs of emulsions were obtained using an optical microscope (Axiovert 200, Zeiss, Toronto, Canada) equipped with a video

camera and a computer. The emulsion sample was taken to a glass slide and the images were taken under light.

3.3 Coalescence Time Measurement by Integrated Thin Film Drainage Apparatus (ITFDA)

To investigate the interfacial property changes of the asphaltene film by adding EC at the oil-water interface, custom-made Integrated Thin Film Drainage Apparatus (ITFDA) was used to measure the real water droplets coalescence. The details on the instrument setup and applications were provided in a previous publication.[65] The ITFDA equipped with a bimorph force sensor, a computer-interfaced video capture device and a data acquisition system was used to measure the coalescence time of two water droplets in oil phase after aging. Figure 3-2 shows the schematic instrument configuration of ITFDA.

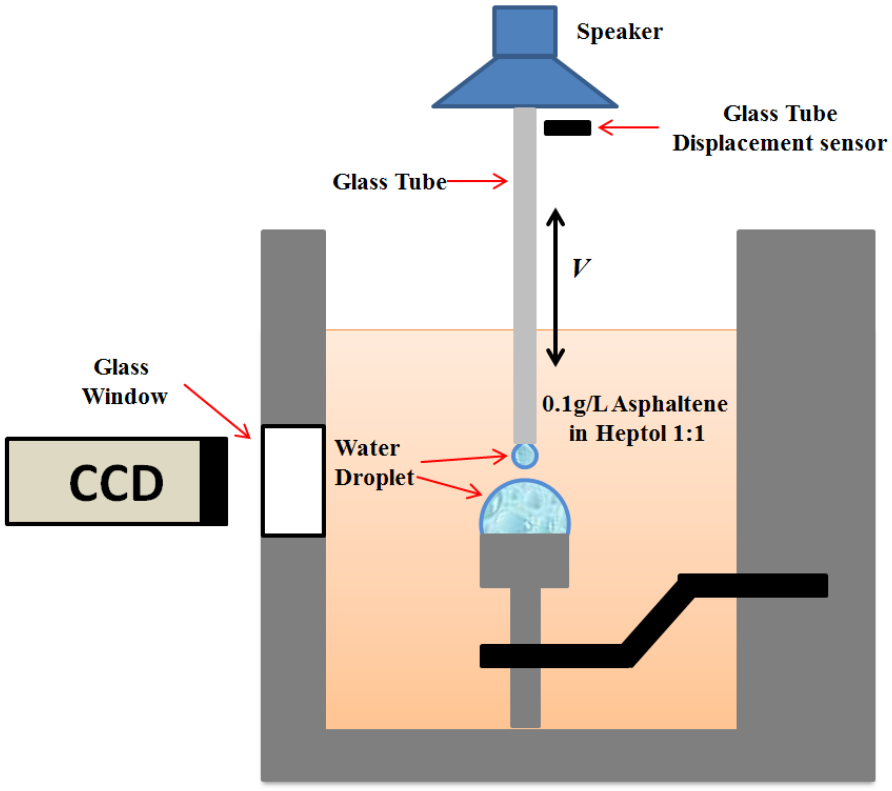

Figure 3-2 Schematic instrument configuration of the integrated thin film drainage apparatus (ITFDA)[65]

The top droplet with a size of ~2.2 mm in diameter and the bottom droplet with ~7.5 mm in diameter were first held apart at a separation distance of ~0.25 mm. Both the top and bottom droplets were aged in the oil phase for 15,000 s. In this study, after 15,000 s aging, 0.2 ppm, 0.5 ppm and 1 ppm EC (based on the mass of heptol phase) was injected respectively drop-wise to the oil phase and diffused for 1 min. The top droplet which was fixed on the capillary was then slowly approached the bottom droplet on the holder in 20 s until the two droplets overlapped for 140 μm. The total approached velocity was 70 μm/s. The contact time of two droplets was set to 200 s. The experiment was conducted at room temperature (23℃). The experiment was recorded by the video capture device frame by frame so that the drop-drop contact and coalescence time can be accurately measured.

3.4 Interfacial Tension Measurement by Drop Shape Analyzer

The dynamic interfacial tension as a function of time in the absence and presence of asphaltenes and EC at the heptol-water interface was measured to study the adsorption kinetics, by the usage of pendant drop technique (Theta Optional Tensiometer, Attension, Biolin Scientific, Finland). A gastight syringe [500 μL] (Hamilton Co., USA) with an 18-gauge needle was used to make an 8 μL water droplet. The needle was submerged in the asphaltene solution (0.1g/L asphaltenes in 1:1 Heptol) until the tip was visible in the frame of capture. The image capture software started measuring and collecting images at 1 Fps when the drop is out. Edge detection method was used to identify the shape of the water droplet and the interfacial tension would be probed by the equation below

$$\gamma = \Delta\rho g \frac{R_0^2}{\beta} \qquad (3\text{-}1)$$

where γ is the interfacial tension, Δρ is the density difference between fluids, g is the gravitational constant, R_0 is the radius of the droplet at apex and β is the shape factor defined through Young-Laplace equation.[36] Interfacial tension of 0.1

g/L asphaltenes was first measured without EC. Total aging time was 20,000 s (5.56 h) for all the systems, equivalent to the aging time used in the interfacial rheology measurement. 0.2 ppm, 0.5 ppm and 1 ppm of EC were injected to the oil phase respectively over 15,000 s and the changes of interfacial tension were recorded afterwards for 5,000 s. The interfacial tension of pure EC at the same concentration was also measured for comparison.

3.5 Dilatational Rheology by Pulsating Drop Method

The dilatational rheology was used to investigate the dynamic characteristics of interfacial films. Dilatation rheology experiments were conducted by the pulsating drop module of OneAttension Optical Tensiometer (PD200). This module enabled the perturbation of a pendant drop. The amplitude, frequency and drop size of the sinusoidal oscillation were captured by the OneAttention Theta software. The droplet size, volume and surface area could be analyzed by the pendant drop method according to the Young-Laplace equation[66] to extract interfacial tension. The change of area (A) and interfacial tension (γ) of the pendant drop is related by a complex surface dilatational modulus, defined as

$$|E| = \frac{d\gamma}{d\ln A} \tag{3-2}$$

From the phase angle difference δ between the interfacial tension and drop area oscillations, the elastic and viscous moduli can be calculated by

$$E'' = |E|\ \sin\delta, E' = |E|\cos\delta \tag{3-3}$$

The oscillating drop technique was used to measure the surface dilatational elasticity. A small drop was formed at the end of the capillary tip and a membrane in the PD 200 module was used to create the harmonic oscillation to measure the surface dilatational elasticity at various frequencies. Figure 3-3a and Figure 3-3b show sample response of interfacial tension and water droplet area

for a pendant drop and sample adsorption kinetics of a surfactant on a pulsating drop.[67]

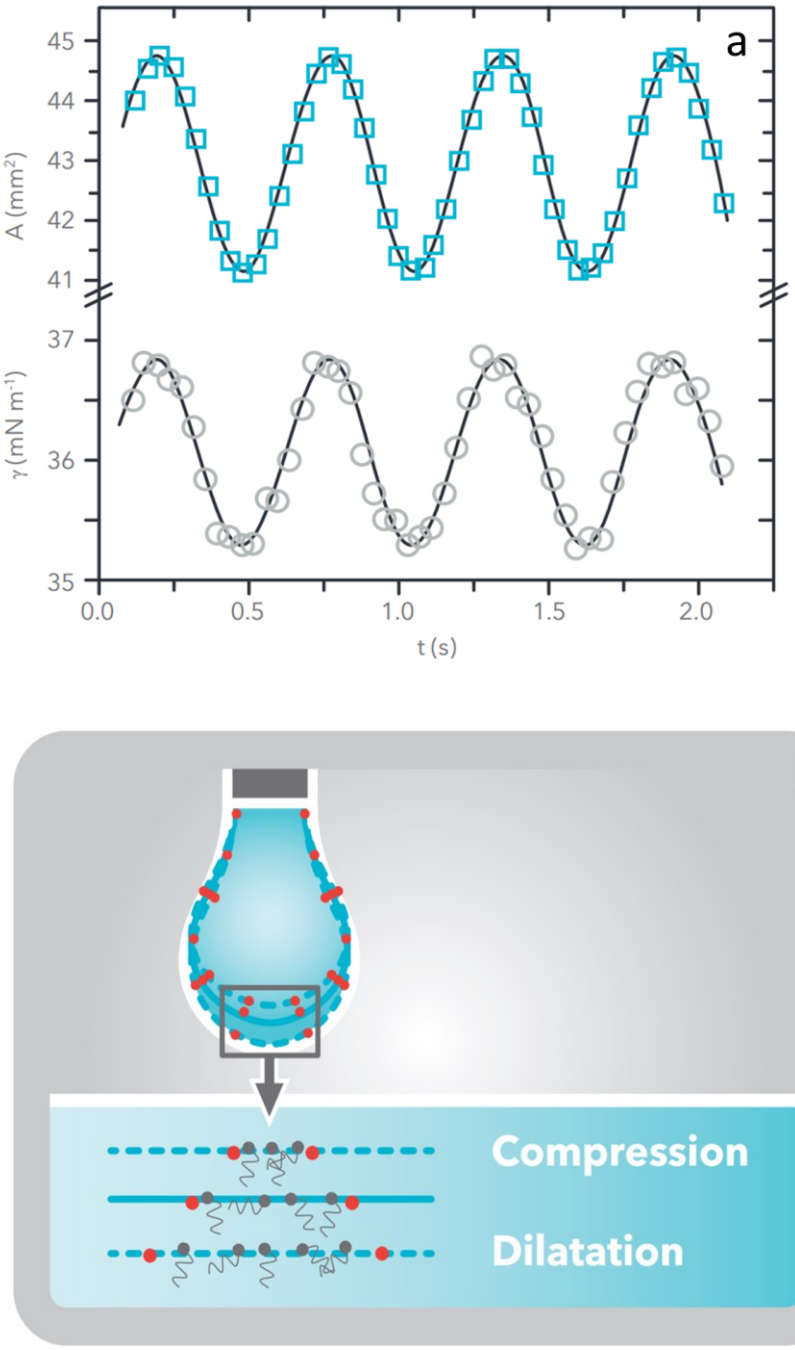

Figure 3-3 Sample response of the interfacial tension and change of water droplet area for a sinusoidal perturbation of a pendant drop (a), and schematic of a surfactant adsorption on a pulsating drop (b).[67]

Sample of 0.1g/L asphaltenes was dissolved in 1:1 Heptol as oil phase. The experiment was run with a 5 µL drop volume at 0.1 Hz frequency and 1.0 amplitude oscillations (10% of the droplet size). The volume oscillations were performed for 20 cycles at each time point and conducted every 10 min. A single water droplet was used for the entire run in order to minimize the drop-to-drop variations that may occur. 0.2 ppm, 0.5 ppm and 1 ppm of EC were injected to the oil phase, respectively, at 15,000 s and the changes of dilatational rheology were recorded for another 5,000 s under the same experimental conditions.[64, 68]

3.6 Interfacial Shear Rheology by Double-wall-ring Geometry

An AR-G2 stress controlled rheometer (TA Instruments, Canada) was used to measure the shear viscoelastic properties, monitoring the change of the formation and breakdown of the asphaltene interfacial films by the addition of EC. The double-wall-ring geometry was shown in Figure 3-4 and was used in this study. The samples were contained in a Delrin trough and the double wall-ring was positioned at the oil-water interface and connected to the rheometer. The trough was placed on the Peltier heated bottom plate, which could control the experiment temperature. The inner and outer radius of the trough is 31.0 mm and 39.5 mm, respectively, with a total interfacial area of 1882.6 mm^2. Steps are present at the inner and outer sides of the trough to create pinning of the interface and reduce the meniscus effect. A circle shaped Pt/Ir ring with an inner radius of 34.5 mm and the thickness of 1 mm was flamed to remove the organic contaminants prior to its use.

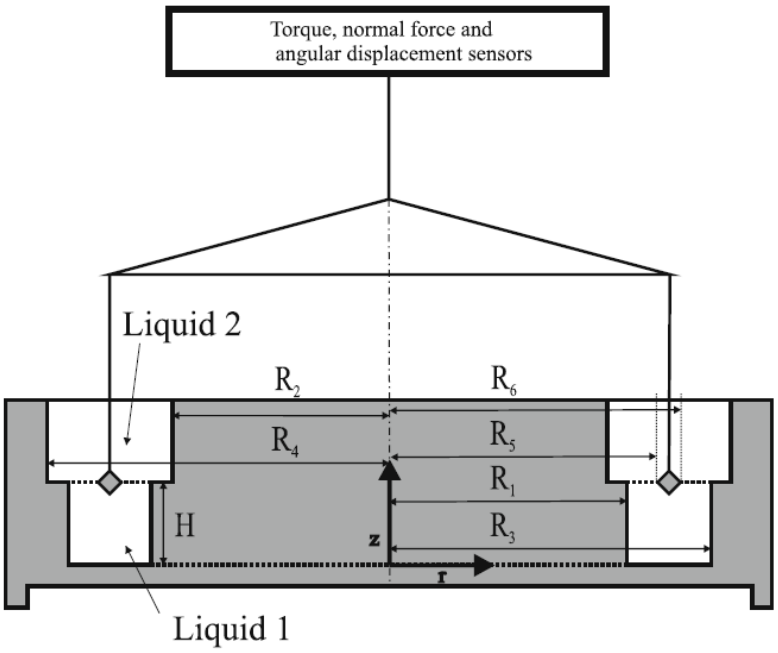

Figure 3-4 Schematic cross section of double-wall-ring setup.[69]

In the interfacial shear rheology, the viscoelasticity of the interfacial film was determined from the harmonic oscillation while the interfacial area is kept constant. In oscillation tests, the sinusoidal shear stress (τ) applied to a surface as a function of time *t* is given by:

$$\tau(t) = \tau_0 \sin(\omega t) \tag{3-4}$$

where ω is the angular frequency. And response (γ) to the sinusoidal shear stress (τ) delayed by a phase angle δ, relative to the generating deformation, i.e.,

$$\gamma(t) = \gamma_0 \sin(\omega t + \delta) \tag{3-5}$$

From the complex shear modulus *G**, the stress and strain can be related as:

$$\tau(t) = G^* \gamma(t) \tag{3-6}$$

*G** can be separated into the real and the imaginary part, corresponding to the storage modulus *G'* and loss modulus *G"*.

$$G^* = G' + iG" \tag{3-7}$$

$G'$and $G^{"}$ are derived from:

$$G' = \frac{\tau_0}{\gamma_0}\cos(\delta) \quad (3\text{-}8)$$

$$G^{"} = \frac{\tau_0}{\gamma_0}\sin(\delta) \quad (3\text{-}9)$$

and represent the elasticity and viscosity of the film, respectively.

The experiment procedure is described as follows. The gap was first zeroed without the ring and then calibrations were conducted before the experiment. The measuring geometry gap was set at 12,000 µm. An aqueous phase of 19.2 mL water was first pipetted to the trough as the subphase. The ring was then lowered to the surface of water subphase. Then freshly prepared 15 mL of 0.1 g/L asphaltenes in 1:1 Heptol solution was poured on the top of the water subphase and a Teflon cap was covered on the trough to prevent evaporation. Oscillatory time sweep measurements were operated at a constant frequency of 0.5 Hz and a strain of 0.8%. All experiments were conducted at 23℃, controlled by a water bath. Duration of these experiments was set to 12 h in total. Dynamic properties of the interfacial asphaltene layer were studied in the region of the linear viscoelasticity. When *G'* reached 1.3 *G"*, 0.2 ppm, 0.5 ppm and 1 ppm of EC were added drop-wise to the top oil phase at around 15,000 s, respectively. The changes of storage modulus *G'* and the loss modulus *G"* were measured afterwards. Detailed procedures of the experiments can be found elsewhere.[63]

3.7 Interfacial Pressure-Area Isotherm

Interfacial Pressure-Area (π-A) Isotherm is a power tool to investigate the compressional behavior of interfacial films. In this case the competitive adsorption of asphaltenes and EC was measured by using a computer controlled Langmuir Interfacial Trough (KSV Instruments, Finland) with a trough area of 17,010 mm^2. The interfacial pressure was monitored by balance using the attached filter paper (Biolin Scientific, product id. KN 0005), known as the Wilhelmy plate.

The interfacial π-A isotherms of three systems were recorded in following three cases: i) asphaltenes in heptol alone; ii) EC in heptol alone; and iii) mixed system of asphaltenes and EC in heptol. The experiments were conducted according to previous published protocols.[57] Prior to its use the trough was thoroughly cleaned with toluene, acetone and Milli-Q® water prior to use until the pressure sensor reached below 0.1 mN/m on the barrier compression of the water phase (120 mL of Milli-Q® water filled as the sub-phase) to 12.5 mm^2. The interfacial pressure was then set to zero, and 100 mL of 0.1 g/L asphaltenes in 1:1 Heptol solution was added on the top of the water phase. After the addition of asphaltenes, the interface was allowed to equilibrate for 30 min during which the asphaltenes adsorbed onto the oil-water interface. Finally the film was compressed to obtain the isotherm of the interfacial asphaltene films. To elucidate the effect of EC on the physical interfacial properties of asphaltene films, EC was added after asphaltene films were formed but before film compression. EC solution was added drop-wise by a Hamilton gastight syringe to the top oil phase at the concentration of 0.2 ppm, 0.5 ppm and 1 ppm, respectively. After 30 min of diffusion, the interfacial pressure was recorded right before compression was started. Also, a control test was taken with pure EC system without the presence of asphaltene films. 0.2 ppm, 0.5 ppm and 1 ppm of EC was added to the heptol top phase respectively and then equilibrated for half hour. The interfacial pressure was recorded right before the compression. All the experiments were performed at room temperature and the interfacial films were compressed at 10 mm/min speed for each barrier.

3.8 Morphology of Asphaltene Film by Brewster Angle Microscopy

The demulsification effect of EC on asphaltene film was further investigated by Brewster Angle Microscope (Model EP3, Accurion GmbH, Germany). Brewster Angle Microscope (BAM) was used to obtain additional information on the properties of interfacial films at the liquid-liquid interface in situ without transferring the film to a solid substrate. Thus, this technique could image the

morphology of asphaltene films at the oil-water interface and the morphological changes of asphaltene films by EC addition in real time to determine the film-breaking mechanisms. A p-polarized light was provided by a standard He-Ne laser with a Glan-Thomason polarizer. The polarizer pointed to a black wedge-shaped reflection plate, which was placed at the bottom of the trough (fixed area of 28 cm^2) to prevent the stray light from the surface. The s-polarized light from the polarizer pointed to the plate at a Brewster's angle, θ_B. At this angle the light can be reflected to the detector from the interface. Hence, the characteristic features of the interface can be recorded by a CCD camera and a 5× microscope with a spatial resolution of ca. 2 μm at the interface. All the images were collected using the EP3View2.x software (Accurion GmbH, Germany).

The experiments were run using the following procedures: 30 mL of water was poured to the trough, followed by gently pipetting 100 mL of oil phase along the sidewall of the trough on to the water subphase. The asphaltene interfacial films were first equilibrated for 15,000 s and imaged at the angle of incidence (AOI) of 42.75° (Brewster Angle), while the polarizer and analyzer were set to around 2° and 10°, respectively. EC4 at the concentration of 0.2 ppm, 0.5 ppm and 1 ppm was added drop-wise and images were taken as the demulsification occurred. In order to elucidate possible dependence between EC concentration and film structures, images were also taken for pure EC4 films. EC solution at the same concentration and volume was drop-wise added to 1:1 Heptol oil phase in the absence of asphaltenes, and images were taken the same way as in the previous description.

3.9 Contraction Behavior of Interfacial Asphaltene Film

The volume contraction experiment is able to quantitatively analyze the skin formation at the surface of water droplet in oil phase. In this study, a pendant drop of water was immersed in dilute asphaltene-in-1:1 Heptol solution. The water droplet with a volume of 10 μl was produced by a gastight syringe [500 μL]

(Hamilton Co., USA) with an 18-gauge needle. The shape and volume of the droplet were maintained to be constant and aged in the oil phase (0.1 g/L asphaltenes in 1:1 Heptol) for a desired duration. The aging was to allow the formation of asphaltene films at the oil-water interface. After aging, the water droplet was retracted manually by the syringe. The crumpling of water droplet might occur during the contraction process. The crumpling ratio, which was the ratio of projected water droplet immediately before crumpling occurred to its initial area, was calculated and recorded as a function of aging time (0.5 h, 1 h, 2h, 3h, 4h, 5h and 6h aging, respectively). Different dosages (0.2 ppm, 0.5 ppm and 1 ppm) of EC were injected drop-wise into the oil phase and the interface was equilibrated for 1 min after 5 h age. The retraction was recorded after each EC addition. A pendant drop technique was used on a drop shape analyzer (Theta Optional Tensiometer, Attension, Biolin Scientific, Finland). The image capture software started collecting images at 1 frame/s speed when the drop is out.

Chapter 4 Dynamic Demulsification Mechanism of Asphaltene-Stabilized Water-in-Oil Emulsions by Ethycellulose

In this chapter, the bottle tests of EC on demulsifying the asphaltene-stabilized water-in-oil emulsions and drop-drop coalescence time measurements were conducted to study the demulsification effect. The interfacially rheological properties of asphaltene interfacial film were analyzed and the results were summarized so as to provide the necessary information for further study on film alteration by EC addition. Then the dynamic demulsification mechanism of EC on the asphaltene stabilized interfacial film was studied systematically. The effect of EC on the viscoelastic properties of the asphaltene film was studied by interfacial shear rheology. The changes of asphaltene film morphology at the oil-water interface were observed in-situ before and after the addition of EC by Brewster Angle Microscope. Dynamic interfacial tensions of asphaltenes, EC and the mixed system were measured to study their adsorption at the oil-water interface by pendent drop technique. Interfacial pressure-isotherm was determined to study the compressional response of interfacial asphaltene films and the effect of EC on disruption of asphaltene interfacial films. The contraction behavior of water droplet in asphaltene oil phase was also studied to determine the film alteration during the demulsification process. Finally, the interfacial dilatational rheology of the asphaltene films was compared with shear rheology as a function of aging time. The effect of EC on the dilatational rheology was also studied to relate the shear rheology with stability of asphaltene films and demulsification performance by EC.

4.1 Demulsification Performance of Water-in-Asphaltene Containing Oil Emulsions

Feng et al. and Hou et al.[41, 58, 70] proved the effectiveness of EC to break up the water-in-diluted bitumen emulsions. Although asphaltene-stablized interface is different from diluted bitumen-water interface, the study of asphaltene systems

allows us to investigate the vital role of asphaltenes in stabilizing emulsions and demulsification of EC on breaking these emulsions.[55] Thus the overall demulsification performance of EC4 was first evaluated by measuring the free water volume resolved from asphaltene-stabilized W/O emulsions. The water-in-asphaltene-containing oil emulsions remained stable for more than 1 day (data not shown) without EC addition. The result of the free water resolved from asphaltene-stabilized water-in-oil emulsions by gravity separation after EC4 addition (free water volume divided by water volume added in emulsions) was recorded for 90 min as shown in Figure 4-1. Free water layer was not observed up to 90 min without EC4 addition because of the stable nature of emulsions. The micrograph of this emulsion captured at 10 min after EC addition is shown on the right side of Figure 4-1. The average drop size was ~25 μm. Dewatering was first observed after 0.1 ppm of EC4 addition, however, free water volume was too small to be measured. Thus water removal for 0.1 ppm EC4 addition was estimated to be 5 %. With 0.2 ppm EC4 addition, the water removal of ~10 % was observed after 5 min of gravity separation. Then the water removal percentage increased to ~20% for the following 30 min and remained constant for another 55 min. The average water droplet size of the emulsion increased slightly to ~37 μm with 0.2 ppm EC addition. Larger water droplets could be observed in the micrograph. With 0.5 ppm EC4 addition, water removal percentage increased from ~14 % to ~34% during the first 35 min of gravity separation and then leveled off at ~34% till 60 min of gravity separation. At 90 min, the removal percentage increased to ~38%, which was much higher than that (20%) with 0.2 ppm EC4 addition. When 1 ppm EC4 was added, water removal increased continuously to ~45% for 90 min gravity separation. The average water droplet size increased dramatically to larger than 100 μm. More water droplets coalesced and formed large water droplets.

Compared to the concentration of EC addition by Feng et al. and Hou et al. (130 ppm),[41, 58, 70] the EC concentration used in this work was much lower. However,

the performance of EC on the asphaltene-stabilized W/O emulsions from the bottle tests results still showed high demulsification efficiency at such low selected concentrations.

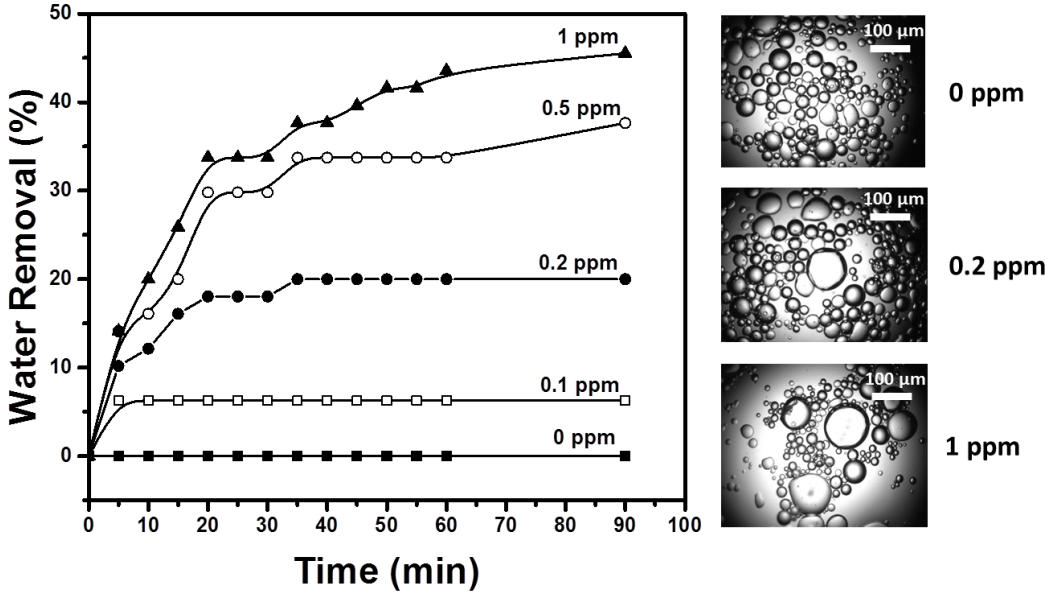

Figure 4-1 Water resolved in bottle tests upon addition of EC at different concentrations (mass based on heptol phase) to asphaltene-stabilized W/O emulsions. Micrographs of water-in-asphaltene-containing oil emulsions with addition of selected EC concentrations (right).

4.2 Drop-Drop Coalescence Time

To further study the role of EC on destabilizing the emulsified water droplets, the coalescence time of two droplets in asphaltene-containing oil phase was determined with and without EC addition. The interfacial rheological response has been previously compared to the emulsion stability measured by bottle tests. However, the systems used in these two techniques are different in surface area to volume ratio and aging mechanisms. Harbottle et al.[63] proposed a coalescence test of two water droplets using our home-made interfacial force balance. Under the promises that the formation of asphaltene films was governed by diffusion-controlled adsorption, the interfacial shear rheology and the emulsion stability

can be directly linked through the drop-drop coalescence time experiment. Previous study showed a shorter coalescence time when viscous contribution dominated the interfacial rheology and a long coalescence time when elastic response dominated the interfacial rheology. In the present study, when EC was applied as a demulsifier, the change of coalescence time was determined to understand the demulsification mechanism.

Coalescence time of two aged water droplets in contact with each other after the addition of EC4 is shown in Figure 4-2. The coalescence time was shown to depend on EC4 concentrations. In the present experiment, the measurement duration was set to 200 s. Two water droplets after aging for 15,000 s in 0.1 g/L asphaltenes /1:1 Heptol solution were brought in contact. Results showed that the two water droplets did not coalesce without EC4 addition after contact for 900 s, considered as stable condition. After 0.2 ppm EC4 was injected, the average coalescence time decreased to 3.29 s. With 0.5 ppm EC4 and 1 ppm EC4 addition, the coalescence time further decreased to 1.38 s and 0.14s, respectively. To improve confidence of the experimental data, each experiment with different EC dosages was repeated for 5 times, and the results were quite consistent with each other.

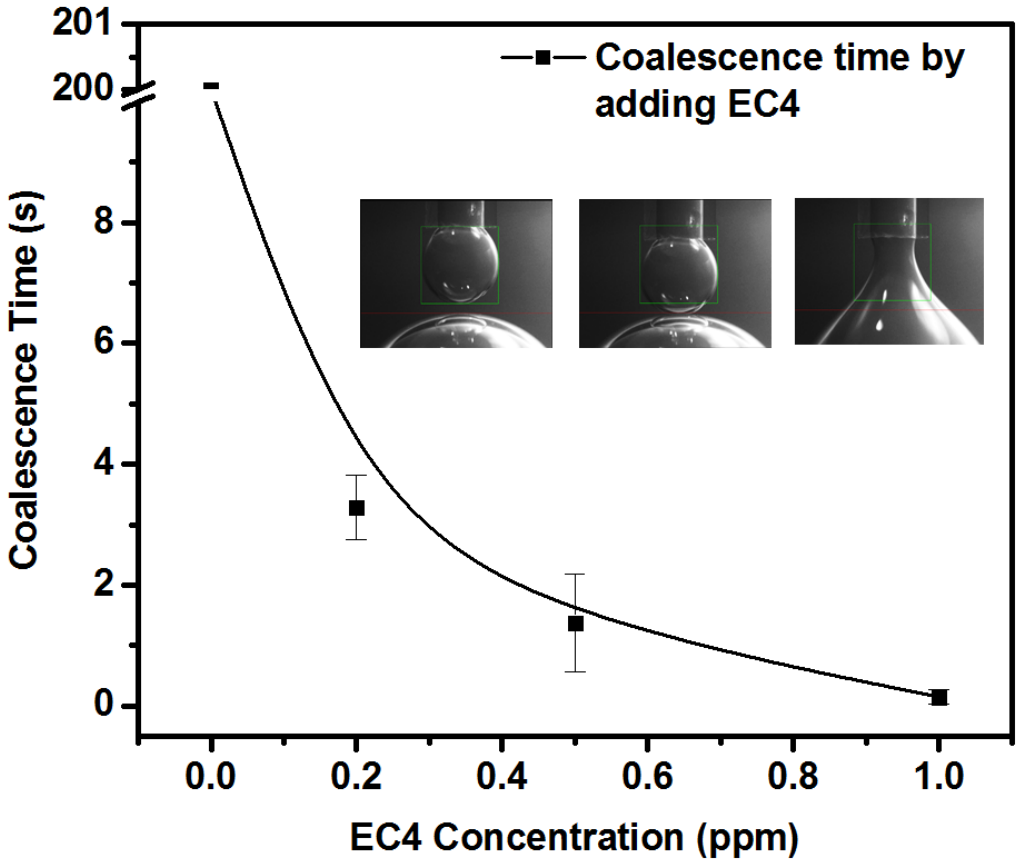

Figure 4-2 Coalescence time for water drops in asphaltene solutions as a function of EC4 at different concentrations (0.2 ppm, 0.5 ppm, 1 ppm), measured after aging in 0.1 g/L asphaltenes/ 1:1 Heptol solution for 15,000 s. Experimental conditions: T= 23℃, $R_{drop\ top}$ ~ 1.09 mm and $R_{drop\ bottom}$ ~ 3.78 mm.

After long time aging of the oil-water interface without EC addition, interfacially active asphaltene molecules could accumulate continuously, cross-link and further form a rigid film which prevents water droplets from coalescence.[56, 59, 63] Thus water droplets did not coalesce while in contact for an extended period of 200 s. The observation from drop-drop coalescence experiments confirmed that the adsorbed asphaltene films could stabilize water droplets in asphaltenes/heptol mixture liquid. When the two water droplets were brought to approach each other, the liquid between the droplets would be squeezed out to the bulk, leading to a thinner film and the inhomogeneous distribution of asphaltenes at the interface. The film thinning can be terminated by relaxation

and reorganization of asphaltenes at the interface. In contrast the addition of EC4 decreased the drop-drop coalescence time from minutes to seconds. In short, the dramatic decrease of drop-drop coalescence time further proves that EC can penetrate into the rigid interfacial film formed by asphaltene adsorption, further break through the hindrance at the interface and promote drop-drop coalescence in asphaltene solution.

4.3 Effect of Demulsifier Addition on Interfacial Rheological Properties

The interfacial rheological response has been previously linked to the emulsion stability measured by bottle tests. However, these two techniques are different on aging mechanisms due to significant difference in volume to surface area ratio of the two systems. Based on almost equivalent surface area to volume ratio, the asphaltene film formation was proven to be governed by diffusion-controlled adsorption and reorganization of the interfacial molecules. Thus we can directly couple the interfacial shear rheology of the asphaltene interfacial film at the oil-water interface and drop-drop coalescence time. In this study, shear rheology of asphaltene films and demulsification of EC was studied by oscillation time measurement. The changes of viscous modulus G" and elastic modulus G' after EC4 addition were measured periodically for 12 h in total, as shown in Figure 4-3a. The amplification of the cross-over region near EC addition is shown in Figure 4-3b.

For 0.1 g/L asphaltene in 1:1 Heptol system, the interfacial film was viscous at 0 s and the viscous modulus started around 4.3×10^{-5} N/m. Then viscous modulus G" began to develop afterwards and the elastic modulus G' became measurable at around 6,000 s. The linear growth of elastic modulus was faster than that of viscous contribution, leading to a cross over at 14, 000 s (G"=G'). Then G' became greater than G" and both moduli kept increasing slowly. G' could be considered as a good indicator of the strong interaction and cross-linking of interfacial molecules.[71] When G'>G", the asphaltene film became elastic dominant. The

intensive interaction and cross-linking of asphaltene molecules make the interfacial film to change from liquid-like to solid-like.[35, 72]

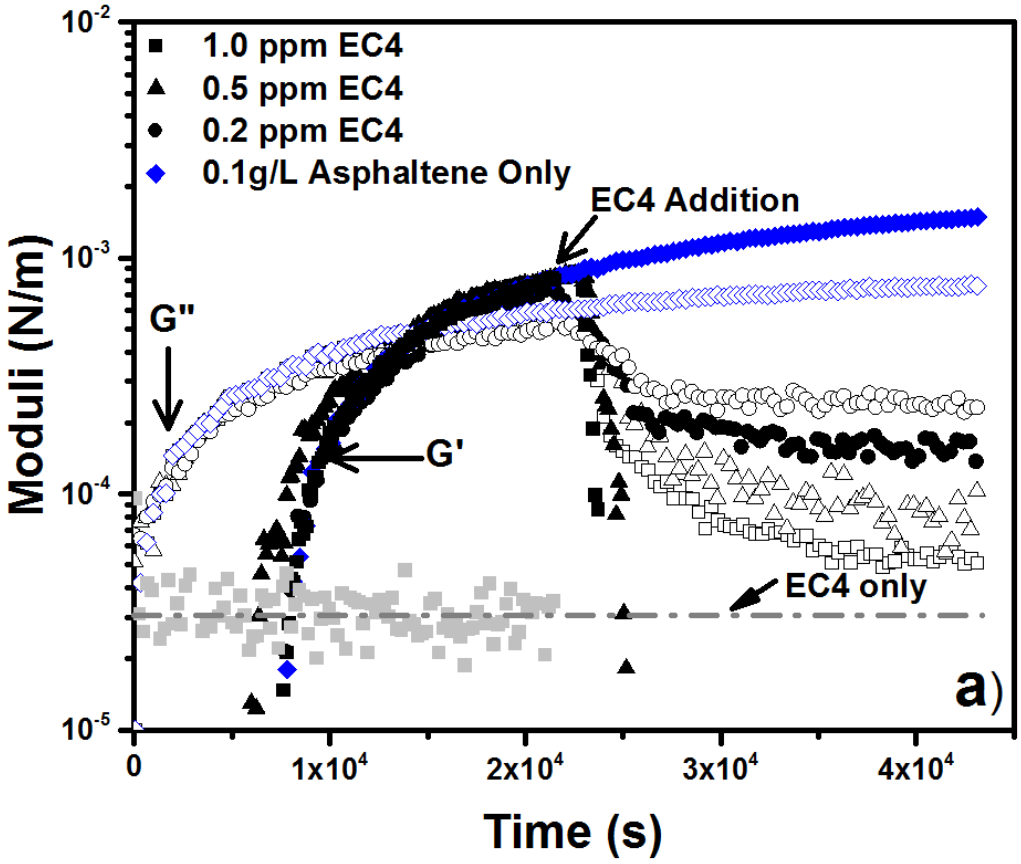

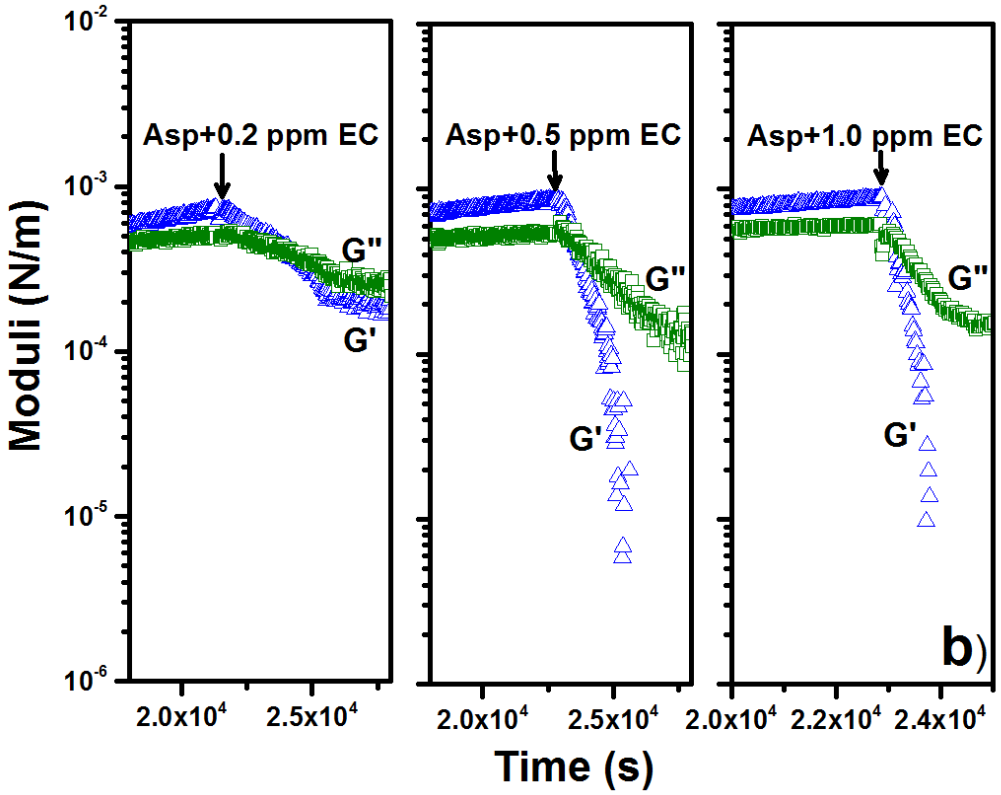

Figure 4-3 Time-dependent viscous (G") and elastic (G') properties of (a) asphaltene films (0.1g/L asphaltenes dispersed in 1:1 Heptol) and effect of EC addition; (b) change of viscoelastic (G' and G") property with EC addition after 5,000 s aging of original asphaltene films. Experimental conditions: strain 0.8%, frequency 0.5 Hz, temperature 23℃. Arrows indicate the addition of EC.

When EC was added at G' ≈ 1.3G" (water droplet turned to be stable from coalescence results), the reductions of elastic and viscous moduli were observed for all three dosages, although to different extents, as shown in Figure 4-3b. After 0.2 ppm EC4 addition, G' turned to be equivalent to G" again at 2,000 s and decreased further below G". The reduction of both G" and G' became slow for 5000 s after EC4 addition, with a value of ~1.2×10^{-4} N/m, in comparison with the initial value of 4.3×10^{-5} N/m. Both G' and G" became plateau afterwards, representing a small change of viscoelastic properties of asphaltenes/0.2 ppm EC4 film with aging. When 0.5 ppm EC4 was added, both G' and G" decreased rapidly, but G' again decreased much faster than G". At 2,500 s the elastic

modulus G' returned to the value of 1.8×10^{-5} N/m, which was close to the original value when it first appeared. Similar to 0.5 ppm EC4 addition, further increasing the EC4 concentration to 1 ppm made the crossover of G' and G" appeared faster at 200 s after EC4 addition. Then G' became lower than G" and both decreased to the original value at 900 s. The change of viscous modulus G" was quite similar to that with 0.5 ppm EC4 addition, but it could drop back to 5.5 $\times 10^{-5}$ N/m, which was close to the start G' value of 4.3×10^{-5} N/m. The G' of asphaltene film with both 0.5 ppm /1 ppm EC4 addition could finally reduce to immeasurable value, suggesting that the strong network of asphaltenes was almost completely disrupted by EC4.

It was demonstrated that EC4 addition was able to decrease both viscous and elastic contributions of asphaltene films. However, the viscous moduli declined at a much slower rate than elastic contributions for all EC concentrations. Only 1 ppm EC addition could lower the viscous response close to original value, showing that the remaining interfacial species were no longer resistant to shear. Also, pure EC4 had a viscous response of ~3.1×10^{-5} N/m. Hence, although viscous moduli of asphaltene films could be reduced by EC4 addition, the reduced values were still higher than those of EC4 alone. These findings indicate that some residual asphaltene molecules were still active at the heptol-water interface, but they could not form a rigid film because of weak interactions. Asphaltenes and EC would form a new co-adsorption film and the weak interaction between these two components of the film was unable to stabilize water droplets coalescence from the emulsions.

The interfacial shear rheology can be linked to drop stability. At the same aging time with G' smaller than G", the drop-drop coalescence time increased with increasing G". Viscosity dominated the microstructure of the interfacial film, corresponding to the short coalescence time on the order of seconds. Beyond the condition of G'>G", the interfacial network was elastic dominant. Under this

condition, the drop-drop coalescence experiments showed the absence of two interacting water droplet coalescence, which was consistent with the implications of interfacial shear rheology results. It was also proven that the viscoelastic response could reflect the film rearrangement with time. The density or strength of asphaltene films is influenced by molecular aggregation and accumulation. By decreasing viscous and elastic moduli with EC addition, water droplets coalesced in less than 4 seconds. The decrease of coalescence time was much faster than the moduli reduction, which further proved that the elastic property of the interfacial film would determine the coalescence of water droplets. The weakened interfacial film by EC addition could no longer prevent the drop-drop coalescence.

4.4 Dynamic Interfacial Tension

To understand the ability of EC to penetrate interfacial asphaltene films and investigate the kinetics of film penetration, the real-time dynamic interfacial tension was measured before (asphaltene aging) and after EC4 addition. As shown in Figure 4-4a, the interfacial tension of 0.1g/L asphaltenes decreased from ~38 to ~25 mN/m over the first 3,000 s. Based on previous studies on adsorption kinetics of asphaltenes at oil-water interface,[36] the rapid change of dynamic interfacial tension at first period of time was controlled by diffusion-controlled kinetics and described by the coupled Gibbs-Duhem and diffusion equation given by

$$\gamma(t) = \gamma_0 - 2RTC\sqrt{\frac{Dt}{\pi}} \qquad (4\text{-}1)$$

where γ is the interfacial tension at time t, γ_0 is the interfacial tension at $t = 0$, R is the universal gas constant, T is the temperature, C is the bulk concentration of the adsorbing materials, and D is the diffusion coefficient. The fast decreasing interfacial tension at early times not only indicates that asphaltenes were interfacially active, but also shows the diffusion-controlled kinetics of

asphaltenes since the interfacial tension varies linearly with $\sqrt{t}$ as shown in Figure 4-4b.

For 3,000 s to 15,000 s of aging, the interfacial tension continuously reduced from ~25 to ~20 mN/m and still did not reach a constant value after 15,000 s. The adsorption of asphaltene molecules became slower than that observed of the first 3,000 s, most likely due to the occupancy of the interface and the further relaxation, rearrangement and reorientation of asphaltene molecules at the heptol-water interface.[73] The trend of decreasing the interfacial tension was quite similar to the increase in the viscoelastic properties of the interfacial films. The adsorption kinetics showed that asphaltenes could rapidly diffuse to the interface and then form a compacted multilayer network, which exhibited as a rigid film.

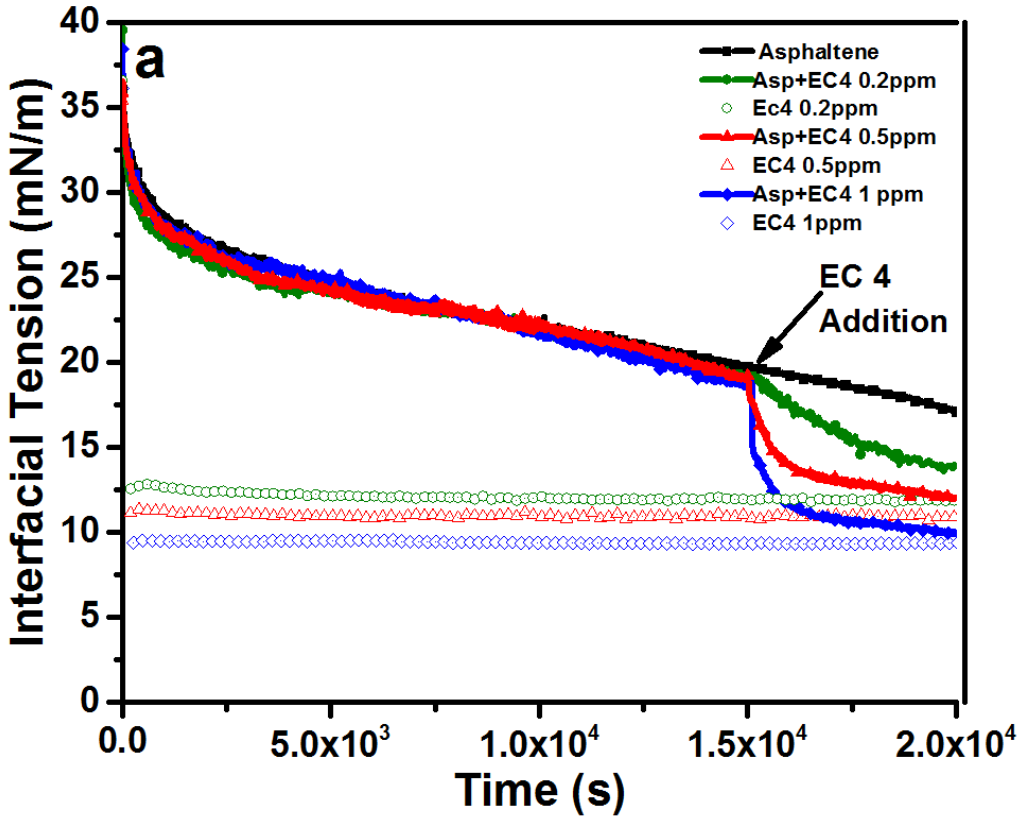

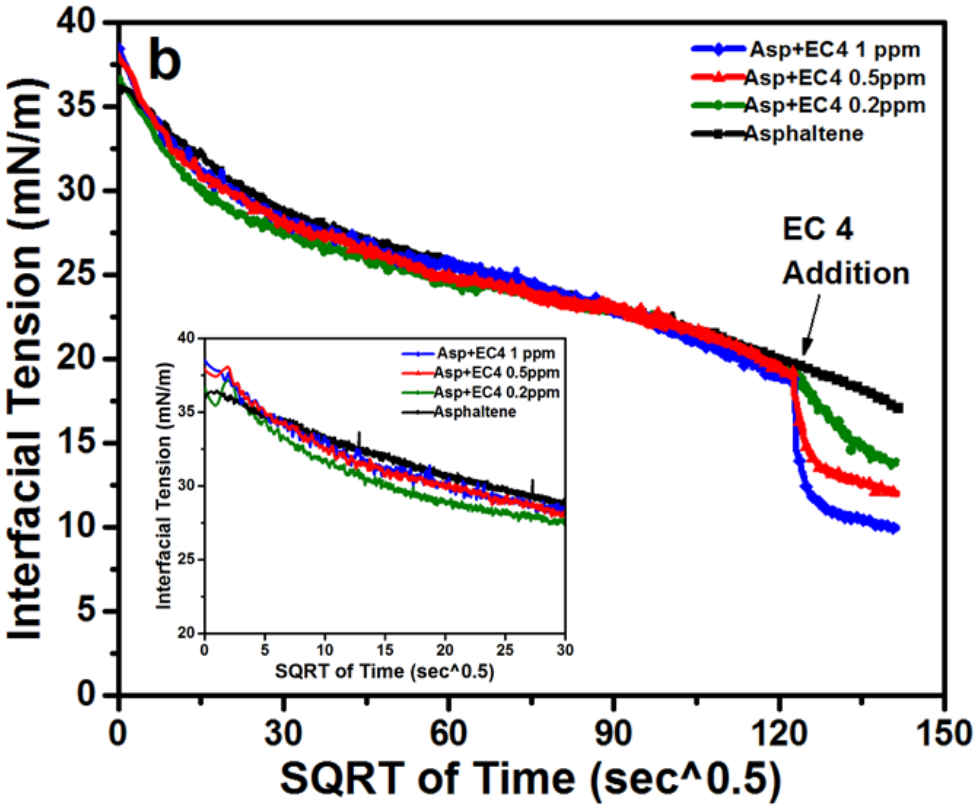

Figure 4-4 Dynamic heptol-water interfacial tension for asphaltenes, pure EC4 and mixed systems as a function of time (a) and as a function of square root of time (b). The arrow in the curve 15,000 s indicates the time when EC4 was injected into the top oil phase.

Based on the aging time needed for stable water droplets, EC4 was added at 15,000 s when asphaltene films formed with high rigidity. It was found that EC4 addition caused rapid decreases for all the interfacial tensions at selected concentrations (0.2 ppm, 0.5 ppm and 1 ppm) in heptol, showing faster kinetics at higher EC4 concentration. Specifically, the interfacial tension decreased slightly from ~20 to ~14 mN/m with 0.2 ppm EC4 addition. The initial interfacial tension reduction scaled almost linearly with $\sqrt{t}$. The interfacial tension of pure 0.2 ppm EC in heptol maintained at ~12 mN/m, which was much lower than that of asphaltenes/0.2 ppm EC4 up to 20,000 s aging. When 0.5 ppm EC4 was added, the interfacial tension decreased from ~20 to 12 mN/m by 5,000 s aging in total. Similar to the reduction scale of interfacial tension of asphaltenes/0.2 ppm EC4

system, 0.5 ppm EC addition to the asphaltene film also showed a rapid linear decrease of interfacial tension with $\sqrt{t}$. The interfacial tension decreased almost to the value of pure EC at the same concentration, with only 1 mN/m higher. This result was quite consistent with the result of interfacial shear rheology measurement that the viscous responses of asphaltene films could not reach to the value of pure EC, indicating EC molecules could not replace all asphaltenes at the oil-water interface. Similar trend could be found in the asphaltenes/1 ppm EC4 system. The interfacial tension first dropped linearly from ~19 to ~11 mN/m as a function of $\sqrt{t}$ over the first 1,500 s and then decreased continuously to ~ 10 mN/m at 20,000 s. The interfacial tension for 1 ppm pure EC4 in heptol maintained constant at a value of 9.4 mN/m, which was very close to the final value of asphaltene systems with 1 ppm EC4 addition. Since EC molecules could irreversibly adsorb to the interface, EC at higher concentration could replace more asphaltenes at the oil-water interface.

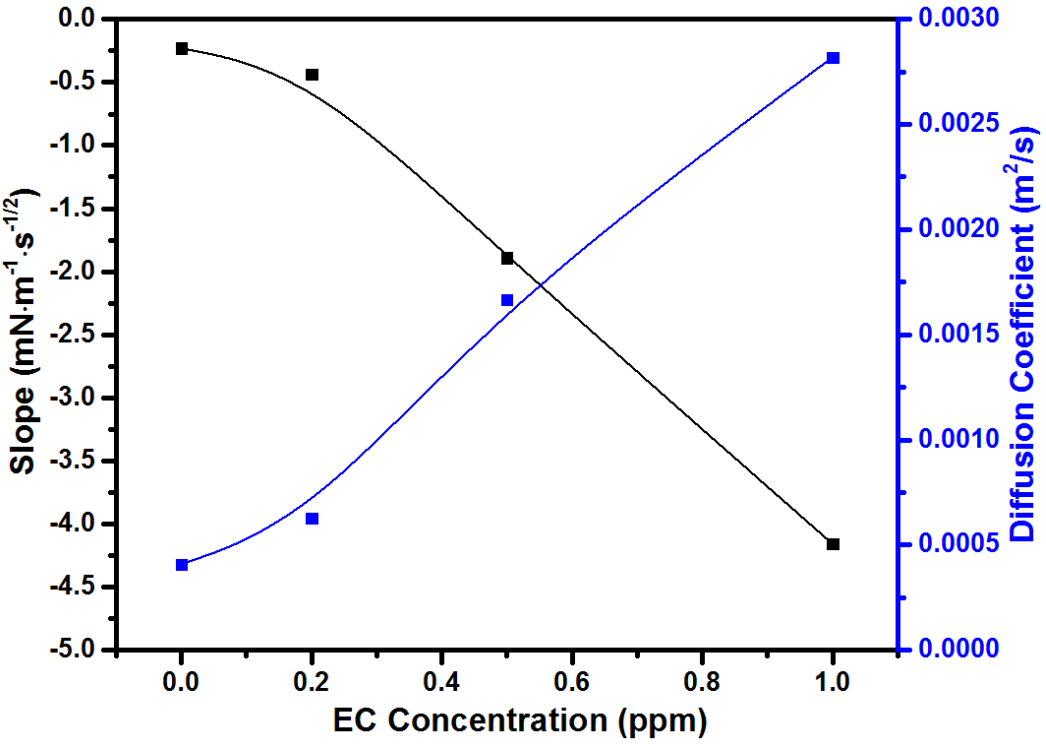

Figure 4-5 Slopes and diffusion coefficients extracted from curves (interfacial tension vs square root time) as a function of EC concentration.

The initial slopes of dynamic interfacial tension were extracted from Figure 4-4b, and the diffusion coefficients were calculated based on equation 4-1. The initial slopes and diffusion coefficients of the mixed systems along with those of pure asphaltene are plotted in Figure 4-5. The initial slope of asphaltenes without EC was determined to be -0.2286 $mN \cdot m^{-1} \cdot s^{-1/2}$. The corresponding values for asphaltenes/EC4 mixed systems were -0.43 $mN \cdot m^{-1} \cdot s^{-1/2}$ (0.2 ppm), -2.55 $mN \cdot m^{-1} \cdot s^{-1/2}$ (0.5 ppm) and -4.83 $mN \cdot m^{-1} \cdot s^{-1/2}$ (1 ppm), respectively. The diffusion coefficient of 0.1 g/L asphaltene in heptol was around 4.08×10^{-4} m^2/s. With EC addition, the diffusion coefficients increased to 6.28×10^{-4} m^2/s (0.2 ppm), 1.67×10^{-3} m^2/s (0.5 ppm) and 2.82×10^{-3} m^2/s (1 ppm), respectively. Based on the results discussed above, we could thus conclude that EC molecules exhibit faster diffusion kinetics than that of pure asphaltenes to the oil-water interface.

Overall, EC4 molecules were much more interfacially active than asphaltenes as shown by lower interfacial tensions, and were able to compete with the asphaltene molecules at the oil-water interface. Also, the penetration of EC to the asphaltene interfacial film occurred and the rigid asphaltene film could be disrupted and broken by EC addition. Since the interfacial tensions for pure EC4 systems dropped in seconds and maintained constant during the entire measurement period, the equilibrium interfacial tensions were obtained.[74] However, the interfacial tensions of asphaltenes after EC4 addition did not reach the equilibrium as in the case of pure EC4, instead the slow decays were similar to the nondiffusion-controlled kinetics of asphaltenes. This result further proves that ECs were not capable of replacing all asphaltene molecules at the oil-water interface, which was consistent with the results of interfacial shear rheology measurement.

4.5 Interfacial Pressure-Area Isotherms

While interfacial shear rheology, coalescence time and dynamic interfacial tension provide the information on the dynamic adsorption and disruption kinetics of the asphaltene stabilized films at the oil-water interface by EC adsorption, the dynamic demulsification mechanism can also be correlated to the compressional behavior of the interfacial asphaltene films. Similar to the interfacial shear rheology contributions, if the compressional responses show low rigidity, water droplets will be unstable and become coalescence rapidly. Therefore the compressional behavior of asphaltenes at oil-water interface was studied by Langmuir interfacial Pressure-Area (π-A) isotherms. In the presence of interfacial materials, the interfacial pressure (π) represents the difference of the interfacial tension (γ) to the clean interface (γ_0), which is given by:

$$\pi = \gamma_0 - \gamma \qquad (4\text{-}2)$$

In this study, γ_0 represents the interfacial tension of a heptol-water interface. When the interfacial materials are diffused to the interface, the interfacial

tension γ will decrease with the interface compression, leading to an increase in the interfacial film pressure π. The compressibility of the interfacial film (C^s) can be defined as

$$C^s = -\frac{1}{A}\frac{d\pi}{dA} \quad (4\text{-}3)$$

where A represents the trough area and $\frac{d\pi}{dA}$ is the slope of the π-A isotherm. The compressional viscoelastic moduli are qualitatively correlated to this slope.[11] The smaller the slope ($\frac{d\pi}{dA}$) is, the more compressive the interfacial film, representing a softer film. On the contrary, a large $\frac{d\pi}{dA}$ represents a small compressibility, reflecting a more rigid interfacial film. The elasticity of the film can be derived from the compressibility of the isotherm.[57] Figure 4-6 shows the comparison of π-A isotherms for asphaltenes, ECs and asphaltenes/ECs films at the oil-water interface. Particularly, the interfacial pressure of asphaltenes alone increased dramatically from 27.6 to 52.1 mN/m by decreasing the interface area from 170 cm^2 to 12.5 cm^2. Since heptane provided a less favorable condition for asphaltene hydrocarbon side chains and promoted the interactions or precipitates of asphaltene molecules,[74] the asphaltene molecules could irreversibly adsorb to the interface and form a very rigid asphaltene interfacial film in short time, leading to a continuous increase in the interfacial pressure of asphaltene films upon compression.

The isotherms of EC4 at different concentration are also shown in Figure 4-6 with π (1 ppm) > π (0.5 ppm) > π (0.2 ppm). The interfacial pressure of 1 ppm and 0.5 ppm EC4 alone had similar absolute value of ~ 40 mN/m, and increased only slightly with reducing the compressional area. The compressibility of these isotherms was large, indicating the EC4 films being extremely soft. Compare to the isotherms of 0.5 ppm and 1ppm, 0.2 ppm EC4 isotherm had a lower interfacial pressure value from 33.9 to 38.2 mN/m with decreasing the interfacial area from 170 cm^2 to 12.5 cm^2. The shape of the isotherm was similar to that of

isotherms at higher EC4 concentration. However the interfacial pressure increase between small and large compressional area was slightly greater. The similarity of these three isotherms could be ascribed to the amphiphilic structures and the interfacial properties of EC. It is shown that even at low concentrations, EC4 molecules still adsorbed to the interface to form an extremely soft network which was much less compressive than pure asphaltene film.

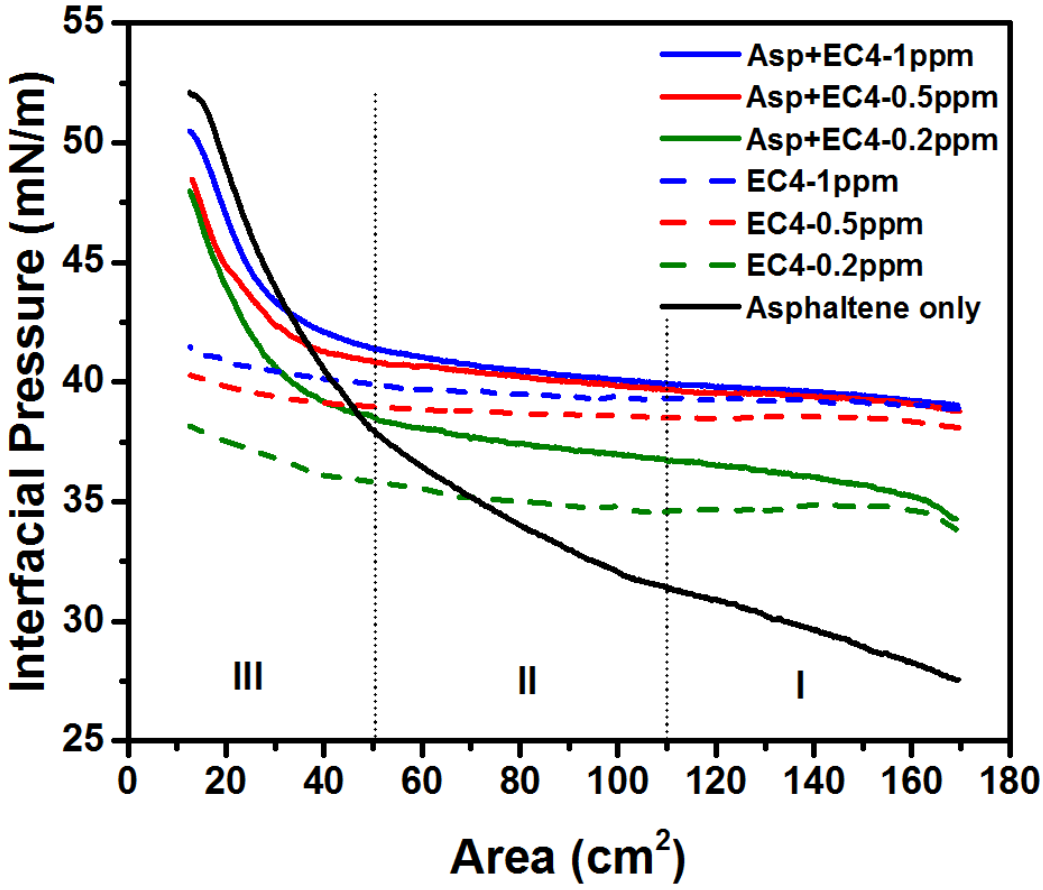

Figure 4-6 Interfacial pressure-area isotherms of asphaltene (100 mL 0.1g/L asphaltenes in 1:1 Heptol top phase), asphaltene/EC (diffusing 0.2 ppm, 0.5 ppm and 1 ppm EC4 solution through 100 mL of asphaltene-containing top phase after 30 min equilibration) and EC interfacial films (diffusing 0.2 ppm, 0.5 ppm and 1 ppm EC4 solution through 100 mL of heptol top phase).

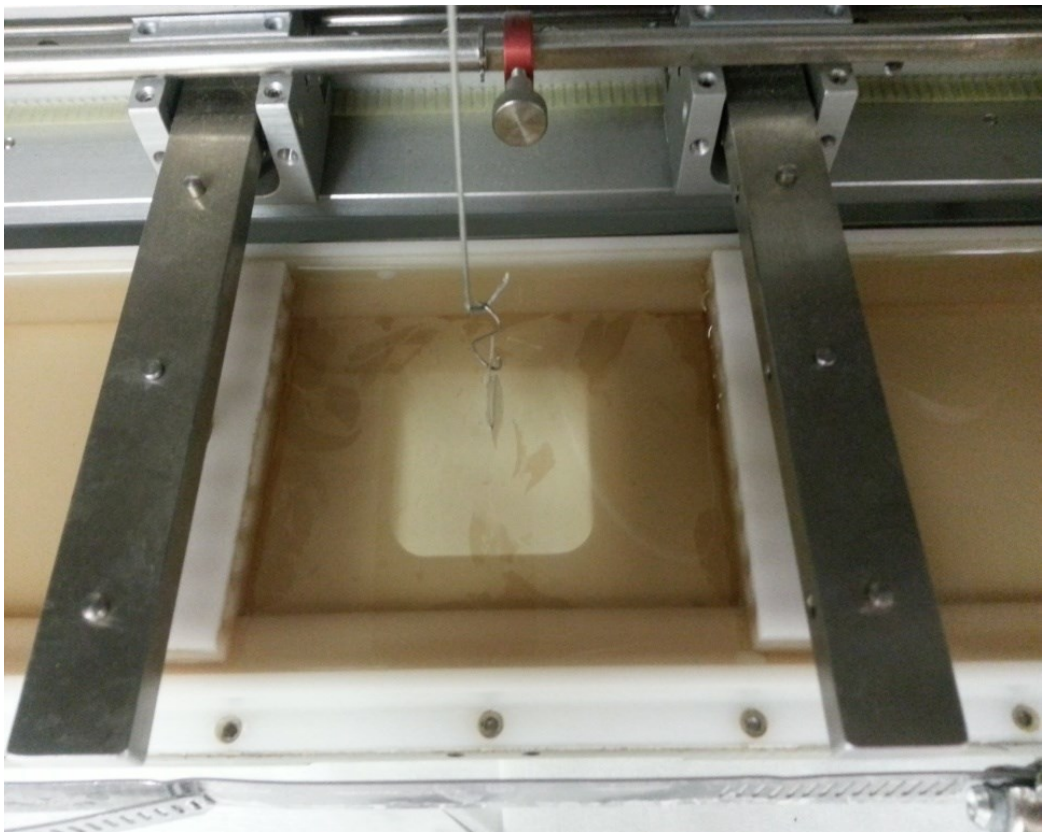

Figure 4-7 Photograph of a 1 ppm EC in asphaltene interfacial film at oil-water interface. Compression area: 50 cm^2.

In an early study, [57] Hou et al. reported quite similar isotherms of asphaltene/EC to that of pure EC interfacial film. However, in Figure 4-6, the compressional behaviors of asphaltene films with EC4 addition were distinctly different from the compressional behavior of asphaltene films or pure EC4 films at the oil-water interface. The entire isotherms could be separated into three compressional regions: (I) from A = 170 to 110 cm^2, (II) from 110 to 50 cm^2 and (III) from 50 to 12.5 cm^2. In the first region (I), the interfacial pressure-area isotherms of asphaltenes with 0.5 ppm and 1 ppm EC4 were mostly overlapped with the isotherms of pure EC4 at the same concentration. The asphaltene films with EC4 addition became soft under low compression. Over this region, EC dominated the interfacial behavior of the asphaltene/EC4 film. This similarity further illustrate that EC4 could penetrate into the asphaltene interfacial film and greatly decrease

the film rigidity due to its stronger interfacial activity. However, for low concentration of EC4 (0.2 ppm), although the asphaltene/EC4 isotherm started at the same absolute value of the isotherm of pure EC at the same concentration, the interfacial pressure kept increasing with decreasing the compressional area, leading to a smaller compressibility of the interfacial film. This result shows that 0.2 ppm EC was not sufficient to replace all asphaltene molecules at the interface over a large interfacial area. In the middle region (II), the interfacial pressure for asphaltene film with 0.2 ppm EC4 addition increased progressively. As the interfacial pressure increased, a co-adsorbed film with both asphaltenes and EC4 was formed at the oil-water interface. The isotherms of 0.5 ppm and 1 ppm EC4 were no longer overlapped with EC4 isotherms, and instead started to increase marginally with reducing the interfacial area under compression. In region (III), the interfacial pressure isotherms of asphaltenes at all EC4 concentrations increased significantly with similar shapes, and finally approached to the isotherms of asphaltene films. The slopes of the curves all increased dramatically, showing interfacial films of much smaller compressibility at the oil-water interface. Over this region, the asphaltene/EC films seemed to be dominated by asphaltenes, leading to the significant increase of rigidity.

Figure 4-7 shows the interfacial asphaltene films after EC addition when the compressional area was decreased to ~50 cm^2. Visually, the asphaltene/EC film appeared as small islands at the oil-water interface. When the interfacial area was decreased to a certain value, small asphaltene islands would compact together to form large films. Under this condition, asphaltenes would dominate the interfacial behavior, and the interfacial co-adsorption film would become partially rigid again. Hence, all results illustrate that EC could penetrate and fracture the asphaltene films, but only partially replace asphaltene molecules at the oil-water interface.

4.6 Morphology of Interfacial Asphaltene Film

Drop-drop coalescence, interfacial shear rheology and dynamic interfacial tension measurements showed that the formation of asphaltene films and the effect of EC were time dependent. In the interfacial pressure isotherms measured by Langmuir trough, the trough area was so large that heptol as the top phase would evaporate very fast. Thus ECs were added only after asphaltene films were aged for 30 min. Based on the results of previous studies, the asphaltene molecules by aging for 30 min could not form an interfacial film of high rigidity. Brewster Angle Microscope (BAM) was able to observe the interfacial asphaltene film at the oil-water interface in situ. An advantage of this technique is the morphological changes of asphaltene films after EC addition could be visualized in real time without disturbing the films. In current study, asphaltene interfacial film was diffused and aged for 15,000 s in order to have a high rigidity. The BAM images in Figure 4-8 provide the characteristics of asphaltene films at the heptol-water interface and changes of morphological features in situ during the demulsification by EC addition. Since the diffusion time of asphaltene molecules to adsorb at the oil-water interface was very long, the asphaltene interfacial film turned to be very thick. Compared to clear heptol-water interface (Figure 4-8f), the asphaltene film appeared as homogeneous network at the interface. This visual observation was in good agreement with the results from the previous discussions. Unlike the asphaltene films, EC film alone (Figure 4-8e) appeared the same as clear heptol-water interface and no EC aggregates could be observed at 1ppm concentration.

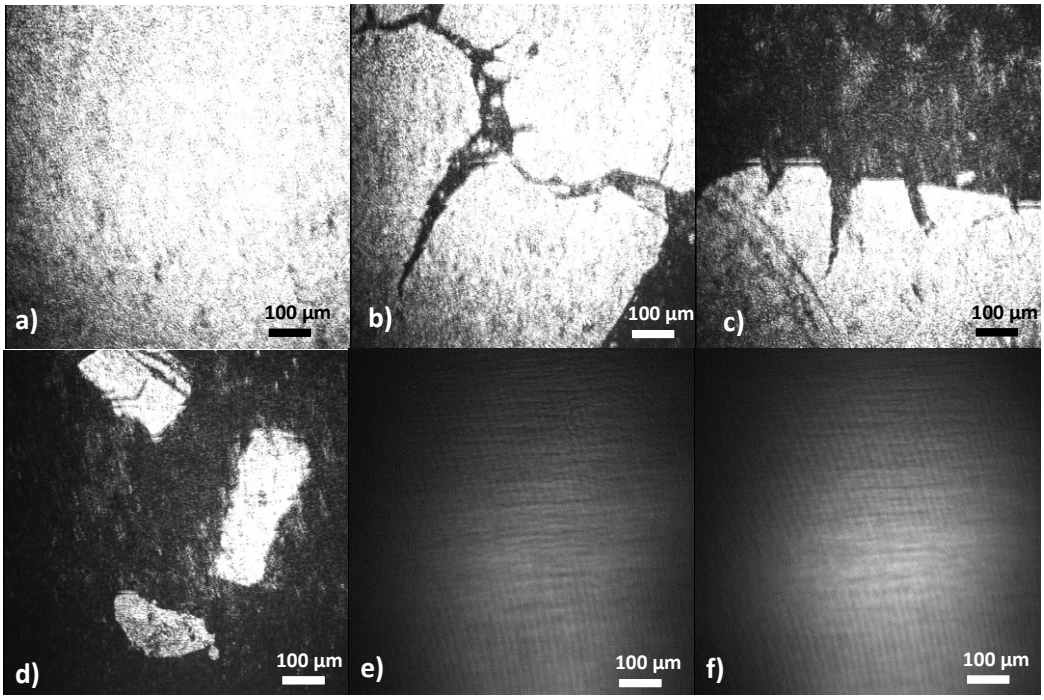

Figure 4-8 BAM images of asphaltene films formed at the oil-water interfaces with EC4 addition. The concentration of EC4 increases in the order of 0 ppm (a); 0.2 ppm (b); 0.5 ppm (c) and 1 ppm (d); in comparison with 1 ppm pure EC film (e) and clear heptol-water interface (f).

With 0.2 ppm EC4 injection from the oil phase to the interface, small irregular cracks appeared on the interfacial films, as shown in Figure 4-8b. The cracks were shown as black areas surrounded by bright asphaltene films. The interface was also observed to change its position and shape to a convex film, as a result of decreasing interfacial tension by EC4 addition. With 0.2 ppm EC4 addition, asphaltene film appeared to be partially broken up by EC4, while majority of the asphaltene film remained unchanged, indicating insufficient EC4 to act on the entire area of asphaltene film at the interface. This finding agrees with the previous discussion that the interfacial properties changed slowly when EC4 concentration was low. When EC4 concentration increased to 0.5 ppm, asphaltene film at the interface started to fall apart to large island-like films which were quite similar to the observation from the Langmuir trough experiments, as shown in Figure 4-7. The edges of these asphaltene islands are

shown in Figure 4-8c. These large island shape asphaltene films were shown as non-uniform, most likely formed by several asphaltene fractures. Further increasing EC4 dosage to 1 ppm further ruptured large asphaltene islands to small pieces of variable sizes and shapes at the oil-water interface. The whole asphaltene film was broken to small asphaltene chunks. The asphaltene molecules displaced by EC no longer stayed at the interface, and instead they went through to the oil phase in the form of asphaltene aggregates.

With EC4 addition, the weak interaction between EC molecules and asphaltenes could form a co-adsorbed film at the oil-water interface. Thus when two water droplets approached in an emulsion, the adsorbed EC4 molecules at the film could bridge the two droplets by their tails, leading to the drop-drop coalescence. The partial displacement of asphaltene films by EC could reduce the coverage of protecting asphaltene film of water droplet at the interface by penetrating into the weak area of the asphaltene network, and hence break the large asphaltene films into micro asphaltene chunks. Thus, BAM images visually proved that EC could irreversibly break down asphaltene films at the oil-water interface, as a result of which the film could no longer prevent water droplet from coalescing in an emulsion.

4.7 Contraction Behavior

Results from dynamic interfacial tension and rheological property measurements proved that both asphaltene and EC molecules could irreversibly adsorb to the oil-water interface. For flat interface, asphaltene films were observed from BAM images to be broken by EC addition. However, the effect of EC on the asphaltene films of water droplet in emulsions has not been investigated before. The incompressible nature of irreversible species could also be studied by deflation behaviour characterized by crumpling. The contraction behavior of asphaltene films at the oil-water interface could reflect the role of asphaltene films to prevent water droplets coalescence in emulsions.[37, 75-76] The volume contraction

experiments of emulsified water droplets in diluted bitumen were designed by Gao et al.[77] to quantitatively analyze the skin formation at the oil-water interface. The steric film had been visualized by the use of micropipette volume contraction method. A crumpling ratio (CR) defined below was introduced to quantitatively analyze the skin formation.

$$\mathrm{CR} = \frac{A_f}{A_i} = \frac{\pi R_f^2}{\pi R_i^2} = \frac{R_f^2}{R_i^2} \qquad (4\text{-}4)$$

where A_i is the initial projected area of the water droplet and A_f represents the projected area of the water droplet right before it crumples. Another microscopic model of emulsion drop system was designed by Asekomhe et al. to directly observe the change of interfacial film.[78] Herein, in the current study, calculating the crumpling ratio from pendent drop enables us to understand the key role of asphaltenes in preventing water droplets coalescence and the effect of EC on demulsification quantitatively.

Water droplets of approximately 2 mm in diameter were aged in 0.1 g/L asphaltenes in 1:1 Heptol. EC solutions at different concentrations were added to the heptol oil phase after 15,000 s. Figure 4-9 shows the images of water droplets captured from the crumpling experiments. The crumpling ratios of these droplets before and after EC addition were calculated and plotted as a function of aging time and EC concentration, as shown in Figure 4-10. Each data point in this figure was calculated by the measurements of three different water droplets and the error bars were the standard deviation of all measurements. When water droplets were retracted without EC addition, the presence of interfacial asphaltene films could be observed at the oil-water interface as wrinkles seen outside these water droplets. A sharp increase of crumpling ratio from 0.2 to 0.43 was found over the first two hours of aging, indicating quick formation of the asphaltene films with time aging. The crumpling ratio continued to increase from 0.43 to 0.52 after another 4 hours of aging, but at a slower rate. The

observed rate of increasing the crumpling ratio was quite consistent with the observed growth of the viscous contribution from the interfacial rheology results. These findings indicate that the aged interfacial asphaltene films are of higher rigidity, leading to a higher crumpling ratio.

The effect of 0.2 ppm, 0.5 ppm and 1 ppm EC4 addition on the crumpling ratio of the water droplets is also shown in Figure 4-10. It was found that the higher, the EC4 concentration, the lower, the crumpling ratio. The trend of reducing the crumpling ratio was shown to be similar to the reductions of dynamic interfacial tension and viscoelastic properties of the interfacial films. This similarity further proves that asphaltene films could be weakened by EC4 addition, and became less rigid. The water droplet in EC-in-toluene solution did not crumple (not shown), since the interfacial film formed by EC4 molecules was very soft. If EC could replace all asphaltene molecules at the interface, water droplets should also not crumple due to the extremely soft interfacial film. The water drop contraction experiments did not shown such trend, indicating that EC4 molecules could only partially replace asphaltene molecules at the oil-water interface. Meanwhile, the crumpling results showed that the remaining asphaltene molecules could still form a less rigid interfacial film at the oil-water interface. These results were quite consistent with the results from previous sections, further proving that asphaltene and EC4 molecules would form a co-adsorbed film at the oil-water interface.

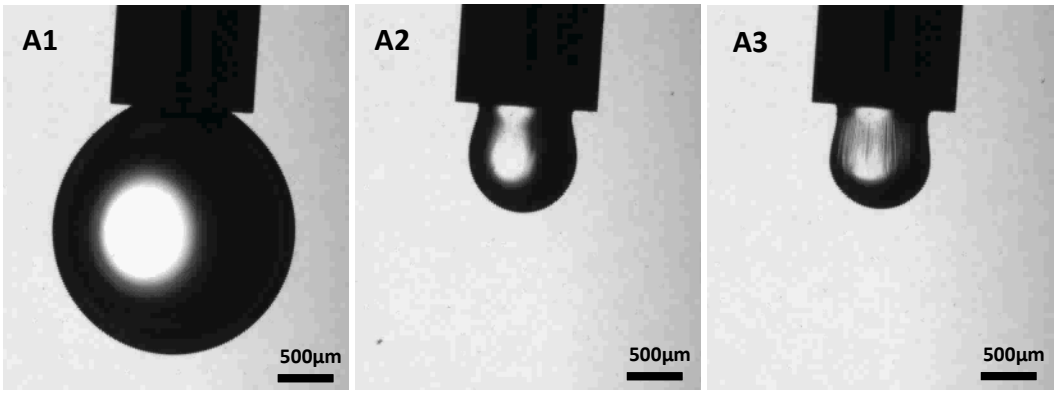

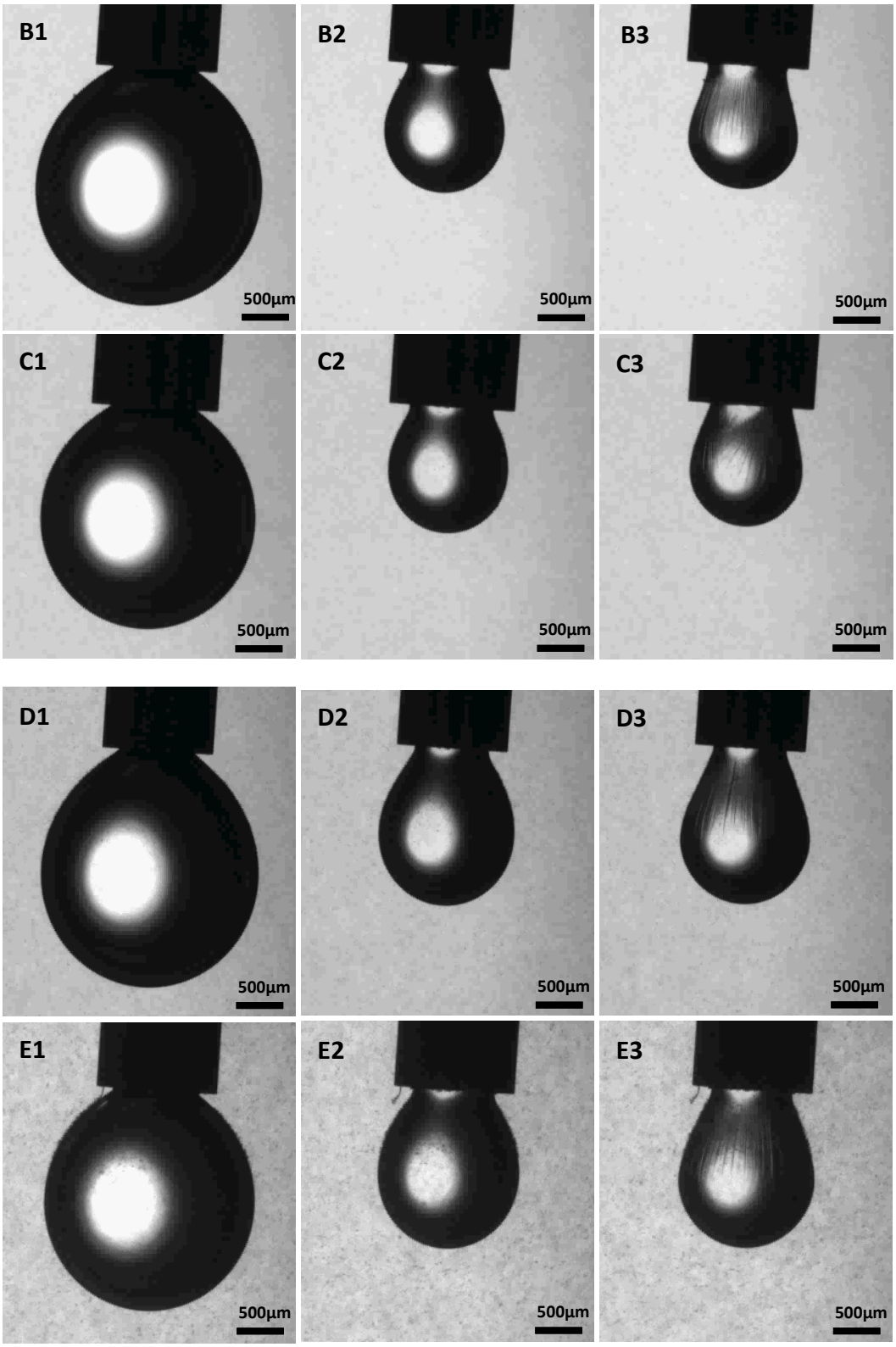
B1
500µm
B2
500µm
B3
500µm
C1
500µm
C2
500µm
C3
500µm
D1
500µm
D2
500µm
D3
500µm
E1
500µm
E2
500µm
E3
500µm

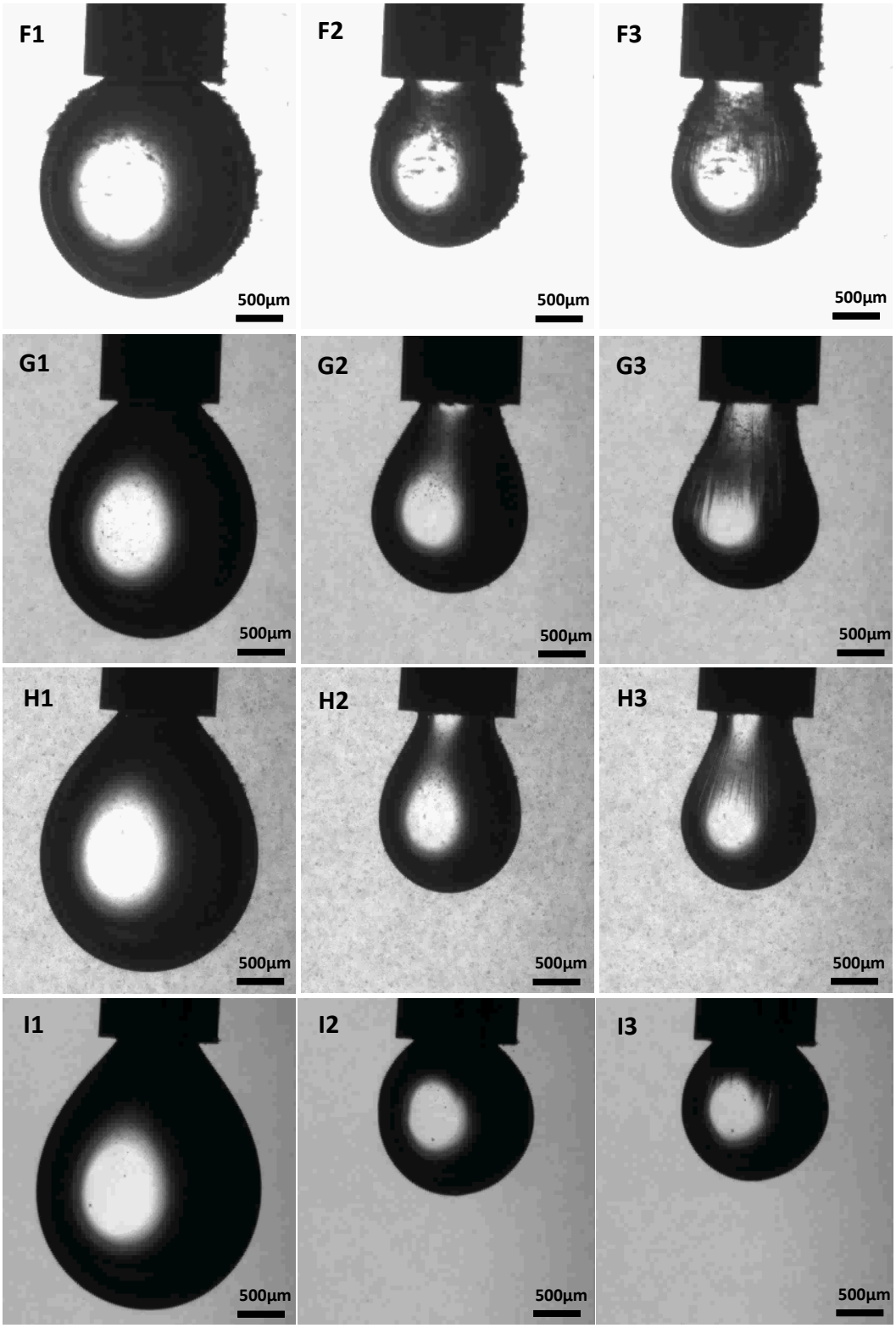

Figure 4-9 Crumpling of water droplets visualized by pendant drop technique. Water droplets age in 0.1g/L asphaltene in 1:1 Heptol for 0.5 h (A1, A2 and A3), 1 h (B1, B2 and

B3), 2 h (C1, C2 and C3), 3 h (D1, D2 and D3), 4 h (E1, E2 and E3) and 5 h (F1, F2 and F3), respectively. 0.2 ppm EC is applied and crumpling ratios are visualized in G1, G2 and G3. 0.5 ppm EC (H1, H2 and H3) and 1 ppm EC (I1, I2 and I3). A1, B1, C1, D1, E1, F1, G1, H1 and I1 are the presentation of the water droplet before retraction. A2, B2, C2, D2, E2, F2, G2, H2 and I2 are the images recorded right before crumpling and A3, B3, C3, D3, E3, F3, G3, H3 and I3 show the images of crumpling first appear.

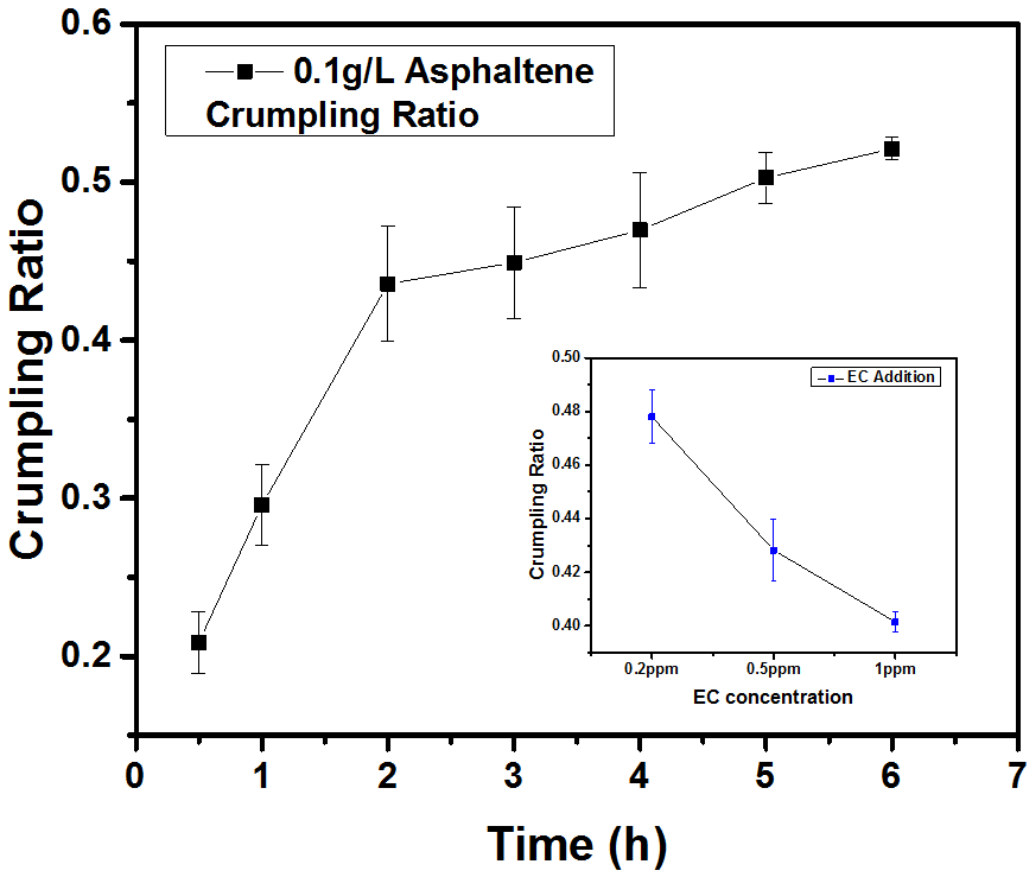

Figure 4-10 Crumpling ratios of water droplets in 0.1g/L asphaltenes in 1:1 Heptol and the effect of EC4 at the concentration of 0.2 ppm, 0.5 ppm and 1 ppm on crumpling ratio.

4.8 Interfacial Dilatational Rheology and Effect of Demulsifier Addition

4.8.1 Interfacial Dilatational and Shear Rheology of Asphaltene Films

Previous studies showed more interests in the dilatational rheology of asphaltene films. The correlation between dilatational rheology and emulsion

stability was proven to be at best qualitatively related, since increasing dilatational elasticity and emulsion stability were in a great agreement. In dilatational rheology, interfacial asphaltene film was dominated by elasticity at short aging time and the dilatational viscosity was unchanged with aging, as shown in Figure 4-11. Such rheological properties were inconsistent with the interfacial shear responses of the asphaltene film.

Both interfacial dilatational and shear rheology can display important interfacial viscoelastic properties of emulsions. The dilatational rheology provides the elasticity of the interface according to the intra and intermolecular interactions and the adsorption of the materials at the interface. The elasticity may have great impacts on the rupture and coalescence of thin liquid films. Whist the interfacial shear rheology measurement showed both the interactions of the adsorbed molecules and the formation of the asphaltene network, which may have had an influence on the thin liquid film drainage.[79] In the asphaltene system, the direct comparison between interfacial dilatational rheology and interfacial shear rheology has seldom been carried out. Rane et al.[68] only correlated the dilatational rheology to dynamic interfacial tension as a function of aging time. To directly compare the interfacial dilatational and interfacial shear rheological properties of asphaltene film at the oil-water interface, they were both plotted as a function of interfacial tension over the same time frame, as shown in Figure 4-11. This was the first time these three techniques were correlated and compared.

Compared to the results of dilatational responses, interfacial shear rheological properties of asphaltene films were found to be more critical to the drop-drop stability.[63] Different from the elastic domination shown from dilatational rheology measurement, the elastic contribution from interfacial shear rheology did not appear when the interfacial tension was higher than 23 mN/m. The interfacial shear rheology showed that the asphaltene film was dominated by

viscous response over short aging time. When the interfacial tension decreased to below 25 mN/m, the elastic modulus from dilatational rheology appeared to reach a plateau, while the elastic response in interfacial shear rheology appeared at an interfacial tension value of 0.029 mN/m and then increased linearly up to interfacial tension value of 0.75 mN/m. Notably, when the interfacial tension decreased to ~20 mN/m, viscous and elastic moduli of shear rheology would crossover and then the elastic modulus would become greater than viscous modulus. This change over indicates that the asphaltene interfacial film transformed from viscous dominant or liquid-like behavior to elastic dominant or solid-like behavior, which agrees very well with the results of drop-drop coalescence time measurement. Hence, the measurement of interfacial properties of asphaltene film by shear rheology was more directly related to the water droplet stability in water-in-oil emulsions.

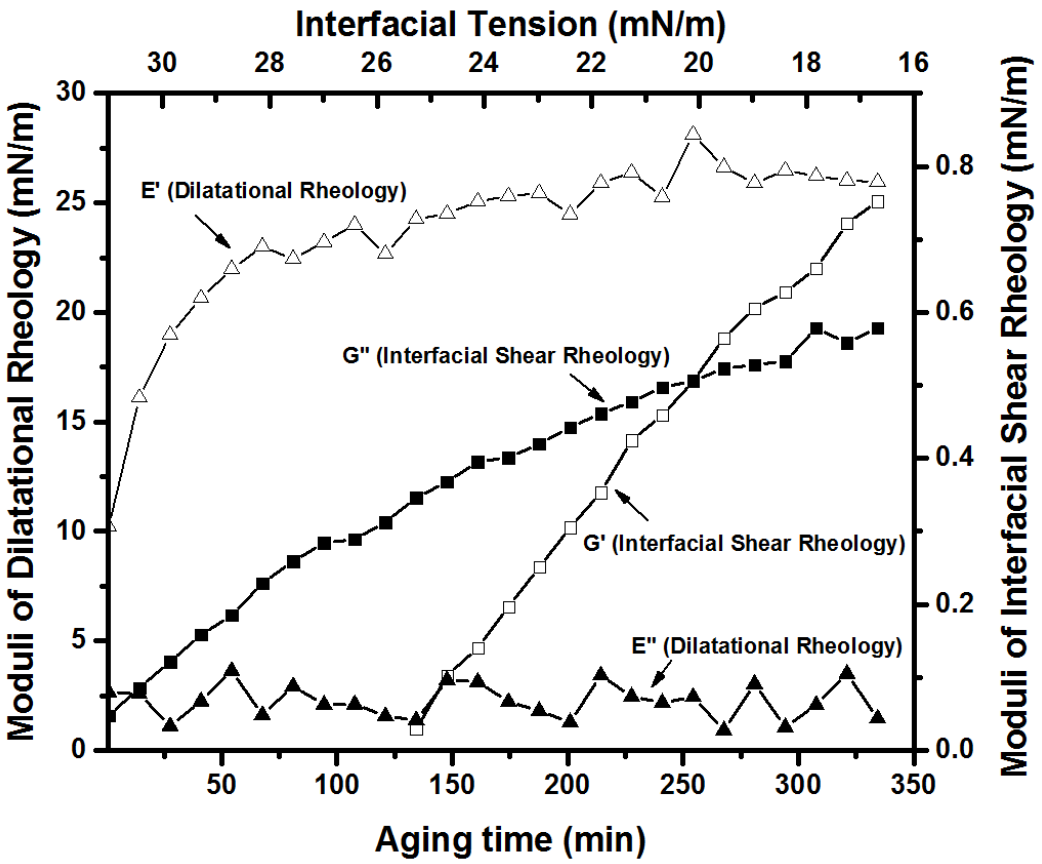

Figure 4-11 Viscous and elastic moduli of dilatational rheology and interfacial shear rheology vs interfacial tension of 0.1g/L asphaltene in 1:1 Heptol. X-axis represents the interfacial tension, Y_1-axis on the left indicates the moduli of dilatational rheology and Y_2-axis on the right shows the moduli of interfacial shear rheology. Experimental conditions of dilatational rheology: frequency= 0.1 Hz, amplitude= 1.0 (10% of drop size), V_{drop} ~ 5 µL and T= 23℃. Experimental conditions of interfacial shear rheology: strain= 0.8%, frequency= 0.5 Hz and T= 23℃.

4.8.2 Effect of EC Addition on Interfacial Dilatational Rheology

The dilatational elastic and viscous moduli of asphaltene with EC additions were also measured as a function of aging time. Since the data points collected before and after EC4 addition showed no differences in the viscous responses as shown in Figure 4-11, the viscous moduli were not discussed here. The results in Figure 4-12 show that with EC4 addition, elastic moduli for all EC concentrations

decreased. The dynamics of decreasing elastic modulus was quite similar to the change in elasticity measured by interfacial shear rheology. Previous studies showed that the asphaltene film with low elasticity would drain faster, leading to a lower stability.[80] EC was able to reduce the strength and thickness of the film and further to destroy the interfacial asphaltene films. However, since the dilatational rheology results could not show significant variation in viscosity of the asphaltene film, shear rheological properties were more convincing to correlate with the drop-drop coalescence and emulsion stability.

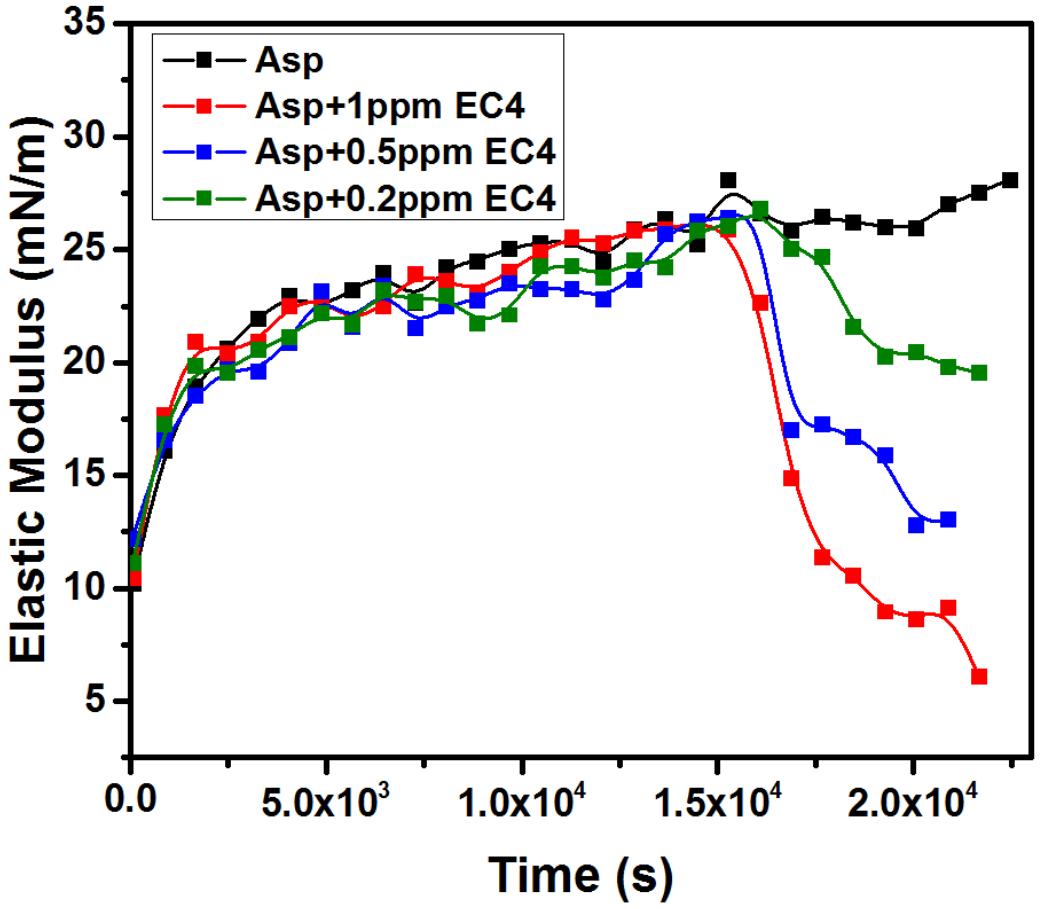

Figure 4-12 Time-dependent dilatational elastic moduli of asphaltenes (0.1g/L asphaltenes dispersed in 1:1 Heptol) and effect of EC addition (0.2 ppm, 0.5 ppm and 1 ppm). Experimental conditions: drop volume 5 µL, frequency 0.1 Hz and 1.0 amplitude oscillations (10% of the droplet size).

Chapter 5 Conclusion and Future Work

5.1 Conclusion

The demulsification performance of EC as a demulsifier in dewatering of the asphaltene stabilized water-in-heptol emulsions was studied by the coalescence time measurements of two water droplets using integrated thin film drainage apparatus and bottle tests. The formation kinetics of interfacial asphaltene films and the effect of EC on demulsification of asphaltene stabilized water-in-oil emulsions were probed by dynamic interfacial tension, interfacial dilatational, shear rheology, interfacial pressure-area isotherms and Brewster Angle Morphology measurements. The results proved that asphaltenes were able to stabilize the water-in-oil emulsions by forming a rigid, solid-like layer at the oil-water interface. Particularly, the rheological properties of the interfacial film showed that when the film microstructure was dominated by the viscous component, drop-drop coalescence time would be quite short; whilst when the elastic contribution dominated, the film network transited to a solid-like state, under which conditions it was quite difficult for water droplets to coalesce. EC could irreversibly adsorb to the oil-water interface by diffusing through the heptol oil phase and partially replace the asphaltene molecules at the interface, leading to a transition from solid-like to liquid-like. As a result, EC can significantly promote the coalescence of water droplets. Due to the penetration of EC into the interfacial asphaltene films and partial displacement of asphaltenes, the fractures of the interconnected network of asphaltenes at the oil-water interface were visualized in situ, further proving the breakdown of the interfacial asphaltene film by EC.

Overall, we brought out the mechanism to understand the dynamical demulsification process of EC from molecular level, which will provide new insights for designing new demulsifier in the future.

5.2 Future Work

Many efforts have been made on revealing the crucial role of EC played during demulsification process. The interaction forces between the two water droplets in asphaltene containing oil and the changes of the forces with the addition of EC during coalescence process should be investigated quantitatively, which could be measured by using Integrated Thin Film Drainage Apparatus.

The asphaltene system used in this work was simple with one concentration in one type of solvent. To gain optimal demulsification effect, it would be quite valuable to explore the influence of concentration of asphaltenes and solvent aromaticity (aromatic/aliphatic ratio) on W/O stability.

It would be economic and environment friendly that demulsifier with low dosage was applied but high quality products could be obtained. Therefore, EC at much lower concentration should be applied to the asphaltene system because of high demulsification efficiency of EC, which would be practical for real industry.

Reference

1. Talk about Oil Sands. http://www.energy.alberta.ca/OilSands/pdfs/FactSheet_OilSands.pdf.

2. Pitts, G., The man who saw gold in Alberta's oil sands. *The Globle and Mail (Toronto)* 2012.

3. *Crude Oil: Forecast, Markets & Transportation*; Canadian Association of Petroleum Producers, 2014.

4. *Energy Resources Conservation Board ST98-2013: Alberta's Energy Reserves 2012 and Supply/Demand Outlook 2013–2022*; 2013.

5. Masliyah, J.; Zhou, Z. J.; Xu, Z.; Czarnecki, J.; Hamza, H., Understanding Water-Based Bitumen Extraction from Athabasca Oil Sands. *The Canadian Journal of Chemical Engineering* **2004,** *82* (4), 628-654.

6. Alberta's Oil Sands: The Facts. http://www.energy.alberta.ca/OilSands/pdfs/AlbertasOilSandsFactsJan14.pdf.

7. Talk about SAGD. http://www.energy.alberta.ca/OilSands/pdfs/FS_SAGD.pdf.

8. Rao, F.; Liu, Q., Froth Treatment in Athabasca Oil Sands Bitumen Recovery Process: A Review. *Energy & Fuels* **2013,** *27* (12), 7199-7207.

9. Long, Y.; Dabros, T.; Hamza, H., Stability and settling characteristics of solvent-diluted bitumen emulsions. *Fuel* **2002,** *81* (15), 1945-1952.

10. McLean, J. D.; Kilpatrick, P. K., Effects of Asphaltene Solvency on Stability of Water-in-Crude-Oil Emulsions. *Journal of Colloid and Interface Science* **1997,** *189* (2), 242-253.

11. Wu, X., Investigating the Stability Mechanism of Water-in-Diluted Bitumen Emulsions through Isolation and Characterization of the Stabilizing Materials at the Interface. *Energy & Fuels* **2002,** *17* (1), 179-190.

12. Yan, Z.; Elliott, J. A. W.; Masliyah, J. H., Roles of Various Bitumen Components in the Stability of Water-in-Diluted-Bitumen Emulsions. *Journal of Colloid and Interface Science* **1999,** *220* (2), 329-337.

13. Madge, D. N.; Garner, W. N., Theory of asphaltene precipitation in a hydrocarbon cyclone. *Minerals Engineering* **2007,** *20* (4), 387-394.

14. Graham, B. F.; May, E. F.; Trengove, R. D., Emulsion Inhibiting Components in Crude Oils. *Energy & Fuels* **2008,** *22* (2), 1093-1099.

15. Kilpatrick, P. K., Water-in-Crude Oil Emulsion Stabilization: Review and Unanswered Questions. *Energy & Fuels* **2012,** *26* (7), 4017-4026.

16. McLean, J. D. S., P. M.; Sullivan, A. P.; Kilpatrick, P. K., *The Role of Petroleum Asphaltenes in the Stabilization of Water-in-Oil Emulsions. In Structures and Dynamics of Asphaltenes*. Plenum Press: New York, 1998; p 377-418.

17. Schramm, L. L., *Emulsions : Fundamentals and Applications in the Petroleum Industry*. American Chemical Society, 1992; p 1-49.

18. Yeung, A.; Dabros, T.; Czarnecki, J.; Masliyah, J., On the interfacial properties of micrometre–sized water droplets in crude oil. *Proceedings of the Royal Society of London A: Mathematical, Physical and Engineering Sciences* **1999,** *455* (1990), 3709-3723.

19. Murgich, J., Intermolecular Forces in Aggregates of Asphaltenes and Resins. *Petroleum Science and Technology* **2002,** *20* (9-10), 983-997.

20. Mitchell, D. L.; Speight, J. G., The solubility of asphaltenes in hydrocarbon solvents. *Fuel* **1973,** *52* (2), 149-152.

21. Zhang, L. Y.; Lawrence, S.; Xu, Z.; Masliyah, J. H., Studies of Athabasca asphaltene Langmuir films at air–water interface. *Journal of Colloid and Interface Science* **2003,** *264* (1), 128-140.

22. Yarranton, H. W., Asphaltene Self-Association. *Journal of Dispersion Science and Technology* **2005,** *26* (1), 5-8.

23. Oliver C. Mullins, E. Y. S., Ahmed Hammami, Alan G. Marshall, *Asphaltenes, Heavy Oils, and Petroleomics*. Springer: New York, 2007.

24. Espinat, D.; Fenistein, D.; Barré, L.; Frot, D.; Briolant, Y., Effects of Temperature and Pressure on Asphaltenes Agglomeration in Toluene. A Light, X-

ray, and Neutron Scattering Investigation. *Energy & Fuels* **2004,** *18* (5), 1243-1249.

25. Kilpatrick, P. K. a. S., P. Matthew, Asphaltene Emulsions. In *Encyclopedic Handbook of Emulsion Technology*, Sjoblom, J., Ed. New York, 2001; p 707−730.

26. Gawrys, K. L.; Blankenship, G. A.; Kilpatrick, P. K., Solvent Entrainment in and Flocculation of Asphaltenic Aggregates Probed by Small-Angle Neutron Scattering. *Langmuir* **2006,** *22* (10), 4487-4497.

27. Fenistein, D.; Barré, L., Experimental measurement of the mass distribution of petroleum asphaltene aggregates using ultracentrifugation and small-angle X-ray scattering. *Fuel* **2001,** *80* (2), 283-287.

28. Eyssautier, J. l.; Levitz, P.; Espinat, D.; Jestin, J.; Gummel, J. r. m.; Grillo, I.; Barré, L. c., Insight into Asphaltene Nanoaggregate Structure Inferred by Small Angle Neutron and X-ray Scattering. *The Journal of Physical Chemistry B* **2011,** *115* (21), 6827-6837.

29. Barré, L.; Jestin, J.; Morisset, A.; Palermo, T.; Simon, S., Relation entre nanostructure des agrégats d'asphaltène et les propriétés macroscopiques de leur solution. *Oil & Gas Science and Technology - Rev. IFP* **2009,** *64* (5), 617-628.

30. Verruto, V. J.; Kilpatrick, P. K., Water-in-Model Oil Emulsions Studied by Small-Angle Neutron Scattering: Interfacial Film Thickness and Composition. *Langmuir* **2008,** *24* (22), 12807-12822.

31. Jestin, J.; Simon, S.; Zupancic, L.; Barré, L., A Small Angle Neutron Scattering Study of the Adsorbed Asphaltene Layer in Water-in-Hydrocarbon Emulsions: Structural Description Related to Stability. *Langmuir* **2007,** *23* (21), 10471-10478.

32. Alvarez, G.; Jestin, J.; Argillier, J. F.; Langevin, D., Small-Angle Neutron Scattering Study of Crude Oil Emulsions: Structure of the Oil−Water Interfaces†. *Langmuir* **2009,** *25* (7), 3985-3990.

33. Yarranton, H. W.; Urrutia, P.; Sztukowski, D. M., Effect of interfacial rheology on model emulsion coalescence: II. Emulsion coalescence. *Journal of Colloid and Interface Science* **2007,** *310* (1), 253-259.

34. Yarranton, H. W.; Sztukowski, D. M.; Urrutia, P., Effect of interfacial rheology on model emulsion coalescence: I. Interfacial rheology. *Journal of Colloid and Interface Science* **2007,** *310* (1), 246-252.

35. Spiecker, P. M.; Kilpatrick, P. K., Interfacial Rheology of Petroleum Asphaltenes at the Oil−Water Interface. *Langmuir* **2004,** *20* (10), 4022-4032.

36. Verruto, V. J.; Le, R. K.; Kilpatrick, P. K., Adsorption and Molecular Rearrangement of Amphoteric Species at Oil−Water Interfaces†. *The Journal of Physical Chemistry B* **2009,** *113* (42), 13788-13799.

37. Yeung, A.; Dabros, T.; Masliyah, J.; Czarnecki, J., Micropipette: a new technique in emulsion research. *Colloids and Surfaces A: Physicochemical and Engineering Aspects* **2000,** *174* (1–2), 169-181.

38. Zhang, L. Y.; Xu, Z.; Masliyah, J. H., Langmuir and Langmuir−Blodgett Films of Mixed Asphaltene and a Demulsifier. *Langmuir* **2003,** *19* (23), 9730-9741.

39. Zhang, L. Y.; Breen, P.; Xu, Z.; Masliyah, J. H., Asphaltene Films at a Toluene/Water Interface. *Energy & Fuels* **2006,** *21* (1), 274-285.

40. Wang, S.; Segin, N.; Wang, K.; Masliyah, J. H.; Xu, Z., Wettability Control Mechanism of Highly Contaminated Hydrophilic Silica/Alumina Surfaces by Ethyl Cellulose. *The Journal of Physical Chemistry C* **2011,** *115* (21), 10576-10587.

41. Feng, X.; Mussone, P.; Gao, S.; Wang, S.; Wu, S.-Y.; Masliyah, J. H.; Xu, Z., Mechanistic Study on Demulsification of Water-in-Diluted Bitumen Emulsions by Ethylcellulose. *Langmuir* **2009,** *26* (5), 3050-3057.

42. Lissant, K. J., *Demulsification: Industrial Applications*. Marcel Dekker: New York, 1983; p 93-132.

43. Oil Demulsification. http://petrowiki.org/Oil_demulsification - Mechanical_methods.

44. Mohammed, R. A.; Bailey, A. I.; Luckham, P. F.; Taylor, S. E., Dewatering of crude oil emulsions 2. Interfacial properties of the asphaltic constituents of crude oil. *Colloids and Surfaces A: Physicochemical and Engineering Aspects* **1993,** *80* (2–3), 237-242.

45. Mohammed, R. A.; Bailey, A. I.; Luckham, P. F.; Taylor, S. E., Dewatering of crude oil emulsions 3. Emulsion resolution by chemical means. *Colloids and Surfaces A: Physicochemical and Engineering Aspects* **1994,** *83* (3), 261-271.

46. *How to Select a Chemical Coagulant and Flocculant*; 1997.

47. Sjoblom, J.; Johnsen, E. E.; Westvik, A.; Ese, M.-H.; Djuve, J.; Auflem, I. H.; Kallevik, H., Demulsifiers in the Oil Industry. In *Encyclopedic Handbook of Emulsion Technology*, Sjoblom, J., Ed. New York, 2001; pp 595-619.

48. Peña, A. A.; Hirasaki, G. J.; Miller, C. A., Chemically Induced Destabilization of Water-in-Crude Oil Emulsions. *Industrial & Engineering Chemistry Research* **2004,** *44* (5), 1139-1149.

49. Kim, Y. H.; Wasan, D. T., Effect of Demulsifier Partitioning on the Destabilization of Water-in-Oil Emulsions. *Industrial & Engineering Chemistry Research* **1996,** *35* (4), 1141-1149.

50. Wu, J.; Xu, Y.; Dabros, T.; Hamza, H., Effect of Demulsifier Properties on Destabilization of Water-in-Oil Emulsion. *Energy & Fuels* **2003,** *17* (6), 1554-1559.

51. Zhang, Z.; Xu, G.; Wang, F.; Dong, S.; Chen, Y., Demulsification by amphiphilic dendrimer copolymers. *Journal of Colloid and Interface Science* **2005,** *282* (1), 1-4.

52. Daniel-David, D.; Le Follotec, A.; Pezron, I.; Dalmazzone, C.; Noïk, C.; Barré, L.; Komunjer, L., Déstabilisation des émulsions eau dans pétrole brut par des polymères siliconés désémulsionnants. *Oil & Gas Science and Technology - Rev. IFP* **2008,** *63* (1), 165-173.

53. Xu, Y.; Wu, J.; Dabros, T.; Hamza, H.; Wang, S.; Bidal, M.; Venter, J.; Tran, T., Breaking Water-in-Bitumen Emulsions using Polyoxyalkylated DETA Demulsifier. *The Canadian Journal of Chemical Engineering* **2004,** *82* (4), 829-835.

54. Kailey, I.; Feng, X., Influence of Structural Variations of Demulsifiers on their Performance. *Industrial & Engineering Chemistry Research* **2012,** *52* (2), 785-793.

55. Pensini, E.; Harbottle, D.; Yang, F.; Tchoukov, P.; Li, Z.; Kailey, I.; Behles, J.; Masliyah, J.; Xu, Z., Demulsification Mechanism of Asphaltene-Stabilized Water-in-Oil Emulsions by a Polymeric Ethylene Oxide–Propylene Oxide Demulsifier. *Energy & Fuels* **2014,** *28* (11), 6760-6771.

56. Rane, J. P.; Harbottle, D.; Pauchard, V.; Couzis, A.; Banerjee, S., Adsorption Kinetics of Asphaltenes at the Oil–Water Interface and Nanoaggregation in the Bulk. *Langmuir* **2012,** *28* (26), 9986-9995.

57. Hou, J.; Feng, X.; Masliyah, J.; Xu, Z., Understanding Interfacial Behavior of Ethylcellulose at the Water–Diluted Bitumen Interface. *Energy & Fuels* **2012,** *26* (3), 1740-1745.

58. Feng, X.; Xu, Z.; Masliyah, J., Biodegradable Polymer for Demulsification of Water-in-Bitumen Emulsions. *Energy & Fuels* **2008,** *23* (1), 451-456.

59. Erni, P.; Windhab, E. J.; Gunde, R.; Graber, M.; Pfister, B.; Parker, A.; Fischer, P., Interfacial Rheology of Surface-Active Biopolymers: Acacia senegal Gum versus Hydrophobically Modifed Starch. *Biomacromolecules* **2007,** *8* (11), 3458-3466.

60. Sun, H.-Q.; Zhang, L.; Li, Z.-Q.; Zhang, L.; Luo, L.; Zhao, S., Interfacial dilational rheology related to enhance oil recovery. *Soft Matter* **2011,** *7* (17), 7601-7611.

61. Mohammed, R. A.; Bailey, A. I.; Luckham, P. F.; Taylor, S. E., The effect of demulsifiers on the interfacial rheology and emulsion stability of water-in-crude oil emulsions. *Colloids and Surfaces A: Physicochemical and Engineering Aspects* **1994,** *91* (0), 129-139.

62. Ekott, E. J.; Akpabio, E. J., A Review of Water-in-Crude Oil Emulsion Stability, Destabilization and Interfacial Rheology. *Journal of Engineering and Applied Sciences* **2010,** *5* (6), 447-452.

63. Harbottle, D.; Chen, Q.; Moorthy, K.; Wang, L.; Xu, S.; Liu, Q.; Sjoblom, J.; Xu, Z., Problematic Stabilizing Films in Petroleum Emulsions: Shear Rheological Response of Viscoelastic Asphaltene Films and the Effect on Drop Coalescence. *Langmuir* **2014,** *30* (23), 6730-6738.

64. Yang, X.; Verruto, V. J.; Kilpatrick, P. K., Dynamic Asphaltene−Resin Exchange at the Oil/Water Interface: Time-Dependent W/O Emulsion Stability for Asphaltene/Resin Model Oils†. *Energy & Fuels* **2007,** *21* (3), 1343-1349.

65. Wang, L.; Sharp, D.; Masliyah, J.; Xu, Z., Measurement of Interactions between Solid Particles, Liquid Droplets, and/or Gas Bubbles in a Liquid using an Integrated Thin Film Drainage Apparatus. *Langmuir* **2013,** *29* (11), 3594-3603.

66. Barnes, G.; Gentle, I., *Interfacial Science: An Introduction*. Oxford University Press: 2005.

67. Interfacial Rheology. http://www.biolinscientific.com/application/interfacial-rheology-measurement/.

68. Rane, J. P.; Pauchard, V.; Couzis, A.; Banerjee, S., Interfacial Rheology of Asphaltenes at Oil–Water Interfaces and Interpretation of the Equation of State. *Langmuir* **2013,** *29* (15), 4750-4759.

69. Vandebril, S.; Franck, A.; Fuller, G.; Moldenaers, P.; Vermant, J., A double wall-ring geometry for interfacial shear rheometry. *Rheol Acta* **2010,** *49* (2), 131-144.

70. Feng, X.; Wang, S.; Hou, J.; Wang, L.; Cepuch, C.; Masliyah, J.; Xu, Z., Effect of Hydroxyl Content and Molecular Weight of Biodegradable Ethylcellulose on Demulsification of Water-in-Diluted Bitumen Emulsions. *Industrial & Engineering Chemistry Research* **2011,** *50* (10), 6347-6354.

71. Fan, Y.; Simon, S.; Sjöblom, J., Interfacial shear rheology of asphaltenes at oil–water interface and its relation to emulsion stability: Influence of concentration, solvent aromaticity and nonionic surfactant. *Colloids and Surfaces A: Physicochemical and Engineering Aspects* **2010,** *366* (1–3), 120-128.

72. Freer, E. M.; Radke, C. J., Relaxation of Asphaltenes at the Toluene/Water Interface: Diffusion Exchange and Surface Rearrangement. *The Journal of Adhesion* **2004,** *80* (6), 481-496.

73. Jeribi, M.; Almir-Assad, B.; Langevin, D.; Hénaut, I.; Argillier, J. F., Adsorption Kinetics of Asphaltenes at Liquid Interfaces. *Journal of Colloid and Interface Science* **2002,** *256* (2), 268-272.

74. Romsted, L. S., *Surfactant Science and Technology*. 2014.

75. Tsamantakis, C.; Masliyah, J.; Yeung, A.; Gentzis, T., Investigation of the interfacial properties of water-in-diluted-bitumen emulsions using micropipette techniques. *Journal of Colloid and Interface Science* **2005,** *284* (1), 176-183.

76. Moran, K.; Yeung, A.; Masliyah, J., The viscoplastic properties of crude oil–water interfaces. *Chemical Engineering Science* **2006,** *61* (18), 6016-6028.

77. Gao, S.; Moran, K.; Xu, Z.; Masliyah, J., Role of Bitumen Components in Stabilizing Water-in-Diluted Oil Emulsions. *Energy & Fuels* **2009,** *23* (5), 2606-2612.

78. Asekomhe, S. O.; Chiang, R.; Masliyah, J. H.; Elliott, J. A. W., Some Observations on the Contraction Behavior of a Water-in-Oil Drop with Attached Solids. *Industrial & Engineering Chemistry Research* **2004,** *44* (5), 1241-1249.

79. Monteux, C.; Fuller, G. G.; Bergeron, V., Shear and Dilational Surface Rheology of Oppositely Charged Polyelectrolyte/Surfactant Microgels Adsorbed at the Air−Water Interface. Influence on Foam Stability. *The Journal of Physical Chemistry B* **2004,** *108* (42), 16473-16482.

80. Kim, Y.-H.; Nikolov, A. D.; Wasan, D. T.; Diaz-Arauzo, H.; Shelly, C. S., Demulsification of Water-in-Crude Oil Emulsions: Effects of Film Tension, Elasticity, Diffusivity and Interfacial Activity of Demulsifier Individual Components and Their Blends. *Journal of Dispersion Science and Technology* **1996,** *17* (1), 33-53.

Appendix

Demulsification Mechanism of High Molecular Weight Ethylcellulose of Asphaltene-Stabilized Emulsions

Introduction

The previous chapters systematically studied the dynamic demulsification mechanism of asphaltene-stabilized emulsions by low molecular weight ethylcellulose (EC4). It has been proven that molecular weight of demulsifier may have great effect on the demulsification efficiency.[1, 2] As a demulsifier, EC is a linear polymer with a six-member-ring repeating units connected by oxygen atom. Feng et al.[3] synthesized a series of EC polymers with different molecular weight and found that high molecular weight ECs had better demulsification performance. Normally, demulsifiers with low molecular weight might have high interfacial activity and are able to adsorb to the interface, leading to the rupture of interfacial film and the coalescence of water droplets in emulsions.[4] On the contrary, the demulsification mechanisms for high molecular weight demulsifiers were based on the water droplets flocculation.[5] In Feng et al.'s study,[6] demulsification performance of EC300 was similar to that of EC4. However the dynamic demulsification mechanism of high molecular weight EC300 has not been studied systematically.

In this chapter, EC300 was used and the dynamic demulsification mechanism was probed to compare to EC4. The performance of EC 300 of asphaltene-stabilized water-in-oil emulsions was studied by bottle tests. The changes of rheological properties and morphology of interfacial asphaltene films by EC300 were studied and a possible dynamic demulsification mechanism could be deducted.

Demulsification Performance of Water-in-Asphaltene-Containing Oil Emulsions

Using bottle tests method, the overall demulsification performance of EC300 was evaluated by measuring the free water volume resolved from asphaltene-stabilized water-in-oil emulsions. The result of the free water removal by gravity separation after EC300 addition recorded for 90 min is shown in Figure A-1. With 0.1 ppm of EC300 addition, the free water removal could reach to ~40%, which was much higher than that of same concentration of EC4. When 0.2 ppm EC300 was added, the water removal increased to ~75 % at 10 min and then turned stable for the following 80 min. With 0.5 ppm EC300 addition, water removal percentage increased dramatically from ~45 % to ~95% for the first 25 min and then reached to ~100%. When 1 ppm EC300 was used, at 5 min after EC addition, water removal increased straightly to 85%. The water removal could increase to 100% by 20 min of gravity separation, indicating almost all water in emulsions could be resolved by EC300.

Compared to the demulsification performance of low molecular weight EC4, EC300 obviously had higher demulsification efficiency at the same concentration. For the highest chosen concentration, EC4 could only resolve 45% of water in the emulsions for the 90 min of gravity separation. In the contrast, EC300 was capable of resolving all emulsified water droplets in the emulsions to free water in 20 min.

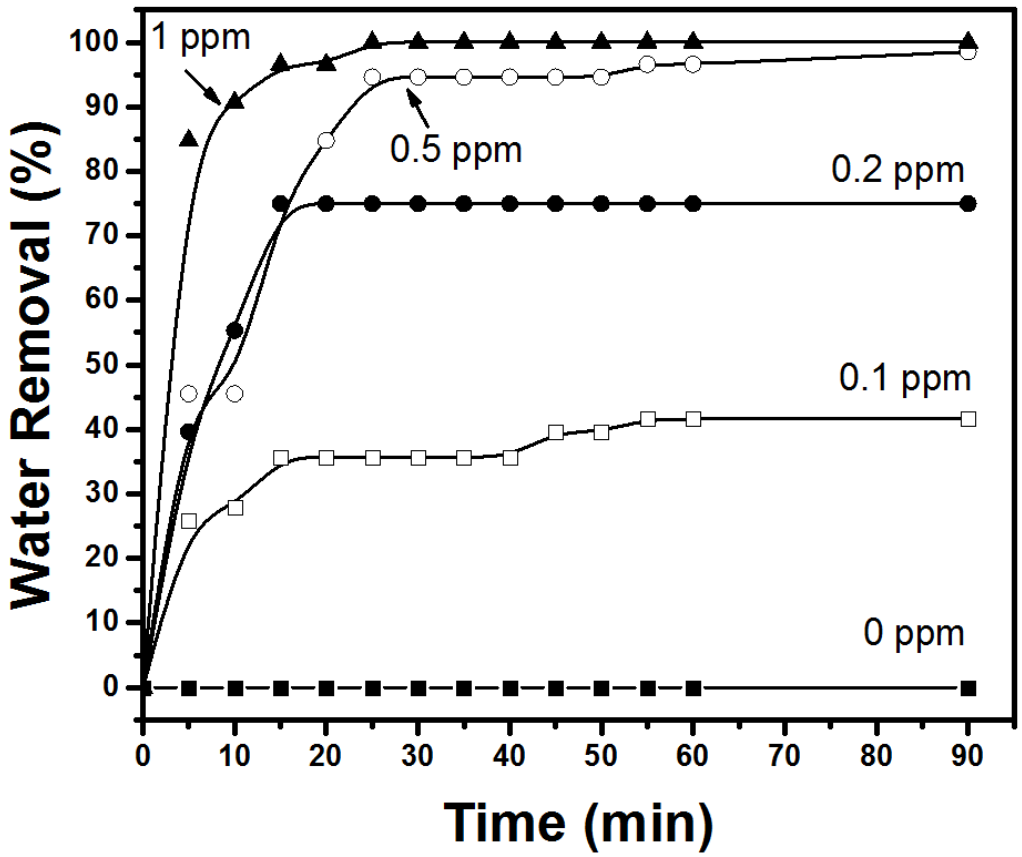

Figure A-1 Water resolved in bottle tests upon addition of EC300 at 0.2 ppm, 0.5 ppm and 1 ppm (mass based of heptol phase) to asphaltene-stabilized emulsions.

Effect of Demulsifier Addition on Interfacial Shear Rheological Properties

Same to the interfacial shear rheology of asphaltene films and the effect of EC4, the viscous modulus (G") and elastic modulus (G') of the interfacial asphaltene film and the changes after EC300 addition were measured periodically for 12 h in total, as shown in Figure A-2. For 0.1g/L asphaltenes in 1:1 Heptol, the viscoelastic properties of asphaltene interfacial films were the same as shown in Figure 4-3a. After 15,000 s, the interfacial asphaltene film turned to elastic dominant structure and changed from liquid-like to solid-like, indicating the formation of strong rigid asphaltene film at the oil-water interface.

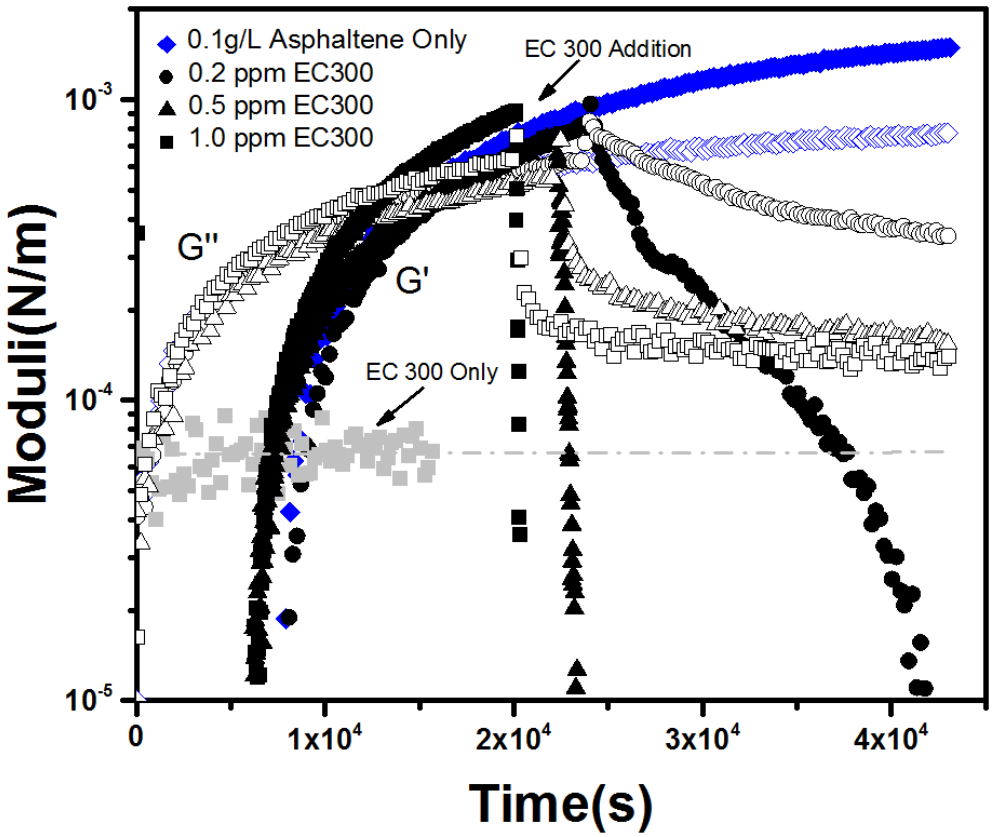

Figure A-2 Time-dependent viscous (G") and elastic (G') properties of (a) asphaltene films (0.1 g/L asphaltenes dispersed in 1:1 Heptol) and effect of EC300 addition at 0.2 ppm, 0.5 ppm and 1 ppm; Experimental conditions: strain 0.8%, frequency 0.5 Hz, temperature 23℃.

When EC300 was added, the reductions of elastic and viscous moduli were similar to those of EC4, with faster reduction of elastic contributions to viscous responses. With 1 ppm EC300 addition, the elastic response decreased dramatically to immeasurable value in 225 s. Similar alteration was found for 0.5 ppm EC300 in 980 s. Compared to the rheological elastic reduction of EC4 (2,500 s and 900 s for 0.5 ppm and 1 ppm respectively), the kinetics for EC300 were much faster. Since elastic response contributes more on the film rigidity, this result further proved that EC300 had higher demulsification efficiency. Different from the elastic change of asphaltene/0.2 ppm EC4 that the elastic modulus curve turned plateaued and could not reached to immeasurable value in the 12 h

measurement, the elastic response of asphaltenes/0.2 ppm EC300 could drop to immeasurable value at 17,716 s (4.9h). Even the elastic deduction decreased very slowly, this result still showed the disruption of interfacial asphaltene film at low concentration EC300.

For the viscosity, none of the viscous moduli of these three EC300 concentrations reached the value of pure EC300 demulsifier. Specifically, although the viscous responses (G") of asphaltene/0.5 ppm EC300 and asphaltene/1 ppm EC300 both decreased quickly at first, they all turned plateaued afterwards. Both of the viscous reductions became quite slow and finally both reached a value of ~1.38 $\times 10^{-4}$ N/m, which was much higher than the pure EC300 viscous response with a value of ~6.78 $\times 10^{-5}$ N/m. When 0.2 ppm EC300 was added, the viscosity of the interfacial asphaltene film did not change as those of higher EC concentration addition. It only decreased slightly from ~6.25 $\times 10^{-4}$ N/m to ~3.52 $\times 10^{-4}$ N/m in total during the measurement. Although the elastic contribution of asphaltenes could be reduced by 0.2 ppm EC300 to immeasurable value, the reduced viscous response was still very high and much higher than pure EC300 viscosity.

Compare to the impact on the interfacial asphaltene film by EC4, the demulsification efficiency by EC300 was much higher on the elasticity. However, the viscous reduction of interfacial asphaltene film by EC300 could not reach to the same level as EC4 achieved. This result further proved the co-existence and co-adsorption kinetics of EC molecules and asphaltene molecules at the oil-water interface. Since the viscous modulus of EC300 (~6.78 $\times 10^{-5}$ N/m) doubled the value of EC4 (3.10$\times 10^{-5}$ N/m), it was reasonable that the overall reduced viscosity of co-adsorption asphaltene-EC300 system was higher than that of asphaltene-EC4. The only difference was that at the first 1,000 s after EC was added, the reduction of viscosity in the case of EC300 was faster than that of EC4, showing faster adsorption kinetics of EC300 than EC4.

These results demonstrate that EC300 could also change the viscoelastic properties of asphaltene films. EC300 addition was capable of effectively decreasing the elasticity of the interfacial asphaltene film from low concentration (0.2 ppm) to high concentration (1 ppm). The higher the concentration, the faster the elastic reduction was. Compared to EC4, EC300 has longer backbone chain and more active amphiphilic groups as well as high viscosity. That is the main reason why EC300 has higher demulsification efficiency on the elasticity and but lower impact on the viscosity of the interfacial asphaltene film.

Interfacial Asphaltene Film Morphology

The images of interfacial asphaltene film and the effect of EC300 are shown in Figure A-3. The image of interfacial asphaltene film at the water-oil interface was the same as shown in Figure 4-8a. Same concentrations of EC300 as EC4 were added and the BAM images were shown in Figure A-3 b-d.

With 0.2 ppm EC300 addition, unlike small irregular cracks appeared on the asphaltene film by EC4 shown in Figure 4-8b, the interfacial asphaltene film started to fall apart and the edges of the asphaltene film island could be visualized in Figure A-3b. When the EC300 concentration increased to 0.5 ppm, the asphaltene film islands further fractured to small asphaltene aggregates. When 1ppm EC300 was added, only asphaltene aggregates could be observed at the interface. These results were consistent with the results in the previous sections that EC300 have higher demulsification efficiency than EC4.

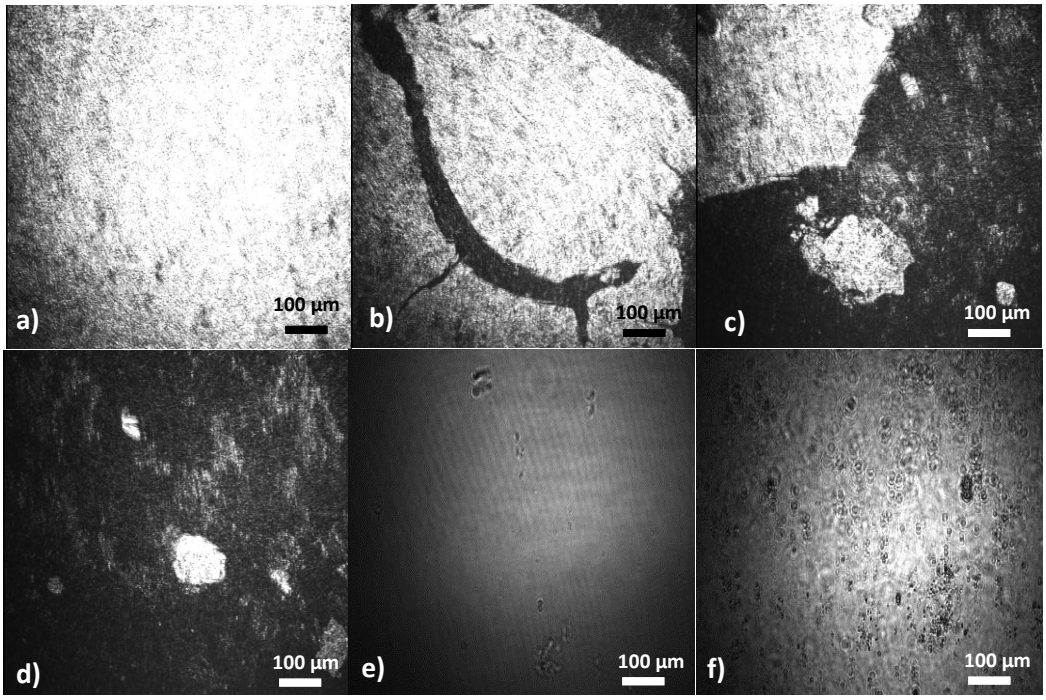

Figure A-3 BAM images of asphaltene films formed at the oil-water interfaces with EC4 addition. The concentration of EC300 increases in the order of 0 ppm (a); 0.2 ppm (b); 0.5 ppm (c) and 1 ppm (d); in comparison with pure EC film at 1 ppm (e) pure EC film at 50 ppm (f).

Besides the different mobility of asphaltene film with the effect of EC300 to those of EC4, the in-situ interfacial film of pure EC showed distinctive film morphology. In Figure A-3e, which showed the heptol-water interface with 1 ppm EC300, EC300 aggregates could be observed at the interface. However, the image of EC4 alone at the same concentration did not show such aggregates. EC300 aggregates could be visualized more clearly if the concentration was further increased to 50 ppm. Due to the amphiphilic structure of EC300 and its high interfacial activity at the interface, EC300 could adsorb to the interface and promote the asphaltene segregation to small domains surrounded by EC.[7, 8] In the rheological measurements, the whole demulsification process might take hours. Thus based on the adsorption of EC300 molecules to the oil-water interface and its high viscosity, it could be explainable that the viscous response in the rheology tests did not decrease very fast as that of elastic contribution.

Reference

1. Shetty, C. S.; Nikolov, A. D.; Wasan, D. T.; Bhattacharyya, B. R., Demulsification of Water-in-Oil Emulsions Using Water-Soluble Demulsifiers. *Journal of Dispersion Science and Technology* **1992,** *13* (2), 121-133.

2. Wu, J.; Xu, Y.; Dabros, T.; Hamza, H., Effect of Demulsifier Properties on Destabilization of Water-in-Oil Emulsion. *Energy & Fuels* **2003,** *17* (6), 1554-1559.

3. Feng, X.; Wang, S.; Hou, J.; Wang, L.; Cepuch, C.; Masliyah, J.; Xu, Z., Effect of Hydroxyl Content and Molecular Weight of Biodegradable Ethylcellulose on Demulsification of Water-in-Diluted Bitumen Emulsions. *Industrial & Engineering Chemistry Research* **2011,** *50* (10), 6347-6354.

4. Sjoblom, J.; Johnsen, E. E.; Westvik, A.; Ese, M.-H.; Djuve, J.; Auflem, I. H.; Kallevik, H., Demulsifiers in the Oil Industry. In *Encyclopedic Handbook of Emulsion Technology*, Sjoblom, J., Ed. New York, 2001; pp 595-619.

5. Peña, A. A.; Hirasaki, G. J.; Miller, C. A., Chemically Induced Destabilization of Water-in-Crude Oil Emulsions. *Industrial & Engineering Chemistry Research* **2004,** *44* (5), 1139-1149.

6. Feng, X.; Xu, Z.; Masliyah, J., Biodegradable Polymer for Demulsification of Water-in-Bitumen Emulsions. *Energy & Fuels* **2008,** *23* (1), 451-456.

7. Feng, X.; Mussone, P.; Gao, S.; Wang, S.; Wu, S.-Y.; Masliyah, J. H.; Xu, Z., Mechanistic Study on Demulsification of Water-in-Diluted Bitumen Emulsions by Ethylcellulose. *Langmuir* **2009,** *26* (5), 3050-3057.

8. Hou, J.; Feng, X.; Masliyah, J.; Xu, Z., Understanding Interfacial Behavior of Ethylcellulose at the Water–Diluted Bitumen Interface. *Energy & Fuels* **2012,** *26* (3), 1740-1745.